Google Embryo for Building Quantitative Understanding of an Embryo As It Builds Itself. I. Lessons from Ganymede and Google Earth

Richard Gordon
Department of Radiology
University of Manitoba
Winnipeg, Manitoba, Canada
gordonr@cc.umanitoba.ca

Abstract
Google Earth allows us to obtain a new vision of the planet we live on, with an ability to zoom in from space to ground level detail at any point on Earth. As it is only recently that we have been able to look toward the Earth from space, we review instead the history of imaging of the Jupiter moon Ganymede, another globe, first seen by Galileo. Observations of Ganymede are mined for lessons on the importance and impact of improving imaging technology. Similarly, new insights may await us when we have proper tools for quantitatively looking at another unexplored globe, the embryo, in a sense for the first time.

Keywords
embryogenesis, Ganymede, Google Earth, history of astronomy, Jupiter, planetary exploration, robotic microscopy

December 6, 2009; accepted January 6, 2010
Biological Theory 4(4) 2009, 390–395.

The Need for Quantification of Embryogenesis

We have hardly begun to look at embryos. Yet we rush ahead with molecular explanations—of what? There is an enormous gap between the genotype and the phenotype, between the so-called blueprint or genetic program of an organism and how it actually builds itself (Gordon 1999). To fill this gap we first need to know what happens, before we try to explain it. That requires observation, the exploratory, often nonhypothesizing, basic work of science, frequently dismissed as "stamp collecting" ("All science is either physics or stamp collecting"—Ernst Rutherford; see Birks 1963), as if theoreticians could reason their way to truth without hard-won data.

We need to observe living embryos developing, with the most sophisticated modern tools we can muster. When things go wrong in embryogenesis, as in birth defects (Gordon 1985; Björklund and Gordon 2006), we need to watch that happen too (Lee et al. 1988). Without quantitative observation (Jacobson and Gordon 1976), all models are handwaving. Without a quantitative match to observation, all models are untested. Without detailed observation of the time course of development before, during, and after experimental manipulation of embryos, crucial data for evaluating models is evaded. Nevertheless we must acknowledge, as we have seen repeatedly in the history of science, that without a working model we scarcely know what observations to make.[1] So in the second part I will show not only beginning steps toward the quantitation of embryogenesis, but also a working model for its spatiotemporal aspects in development (Gordon 2009). Here we will take a step back in time and zoom forward showing how the instrumentation improved that allowed visualization of Ganymede, one of the moons of Jupiter. But let us first look at Earth.

Google Embryo

To consider where I am going with these ideas, here are some of the features and functionalities of Google Earth (Brown 2006; Crowder 2007; Evans and Smith 2007; Kennedy 2009) that are available to anyone with a computer and Internet connection:

1. Center the image on any part of the Earth
2. Zoom in or out relative to that location
3. Overlay maps of roads, elevation, and other features
4. Label interesting places
5. Measure the distance between locations
6. Calculate travel time from one place to another
7. Fly over terrain as if in a helicopter.

With embryos we are dealing with one more dimension—time. It is as if Google Earth were extended to encompass geological events having to do with the tectonic motion of the continents, the movement of ice caps during ice ages, and the rise and fall of sea level and mountain ranges, over millions of years. We need to measure the speed of analogous events on the surface of an embryo, their interactions, and their consequences for normal and aberrant embryo development. We could, for example, center the image on one cell and watch embryological development from the viewpoint, so to speak, of that cell, three dimensionally rotating each surface image in turn so that that cell remains in the center of our view. The whole effort could be called Google Embryo.

Figure 1.
Galileo's telescopes (*Encyclopedia Britannica* 2009; with permission) and his notes on Jupiter's moons (Knowledgerush.com 2003; GNU Free Documentation License).

Observing Ganymede

Imaging crosses all disciplines, and as a once amateur astronomer (Rickey and Gordon 2004), I often look to astronomy for lessons for biology and medicine (Gordon 1978; Gordon and Hoover 2007; Gordon et al. 2007) or vice versa (Gordon and Sinnott 1983). To judge where we are along the pathway toward quantitative imaging of embryos, let's consider the history of observations of the moons of Jupiter, and focus on Ganymede:

> On January 7, 1610 Galileo discovered three of Jupiter's four largest satellites (moons): Io, Europa, and Callisto. He discovered Ganymede four nights later. He noted that the moons would appear and disappear periodically, an observation, which he attributed to their movement behind Jupiter, and concluded that they were orbiting the planet (Kruschandl 2006; cf. Drake and Galilei 1957).

Galileo therefore observed that the Earth was not alone among the planets in having a moon circling it while also circling the sun, thereby removing his one reservation about Copernicus' sun-centered universe (Robison 1974). Galileo's instrument was a simple refracting telescope and he sketched what he saw by hand (Figure 1), mere scratchings that profoundly altered our view of our place in the universe, albeit because most of his successors erroneously presumed that

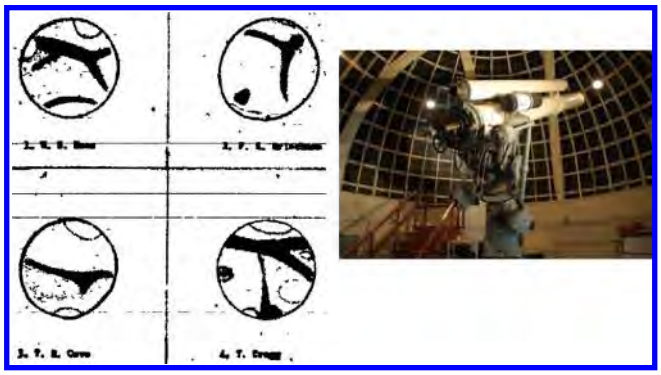

Figure 2.
Ganymede sketched from Earth by four astronomers on the same evening (Haas 1950; with permission of the author and Sky Publishing) with the same 12-inch refractor telescope at the Griffith Observatory (Griffith Observatory 2009; with permission of Cathy Huynh Vo).

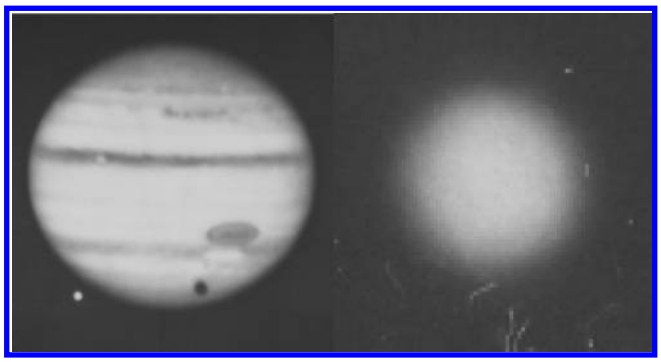

Figure 3.
Jupiter with Ganymede casting a shadow on it, as observed by the 200-inch Earth-based reflecting telescope. No detail shows up on the enlarged image of Ganymede on the right. (Thanks to and with permission of W. Scott Kardel, Public Affairs Coordinator, Palomar Observatory, California Institute of Technology, who scanned the original plate for me.) Jupiter's diameter is 140,000 km, Ganymede's is 5,262 km. For comparison, Earth's diameter is 12,700 km.

Galileo thought he had demonstrated an analogy of the whole solar system (Robison 1974). It is important to note that Galileo saw no details on Jupiter (Hockey 1999), let alone Ganymede.

I skip forward 339 years (a period covered by the Appendix). On the exceptionally atmospherically steady evening of August 23, 1949, four experienced amateur astronomers used the 12-inch refractor at Griffith Observatory (2009) to sketch Ganymede, with deliberate care to observe without influencing one another. The results were bizarrely disparate (Haas 1950) (Figure 2). The slight consistencies between them might be an improvement over a Ganymede image made with the Palomar 200-inch reflecting telescope (Figure 3), though one could question that based on the latter's superior optics. But the human eye with even a modest telescope has an advantage over astrophotography with a larger telescope in that the latter ordinarily averages an image over a time exposure, while the human brain can choose to see detail during the rare moments of atmospheric stability and integrate those into a sketched image. This is perhaps why Figure 3, taken with the largest telescope at the time, can be judged

Figure 4.
Ganymede being occulted by Jupiter, as recorded by the Earth-orbiting Hubble telescope (Weaver et al. 2007; NASA 2009).

inferior to the admittedly disparate images obtained by human vision (Figure 2). For completeness of the history of such drawn images, filling in the huge gap in my story before 1950, John Westfall has compiled a list of many published observations of Ganymede before the first space probe (see the Appendix). Adaptive optics are now used to compensate for atmospheric blurring (Shope and Fisher 1999).

Even the orbiting Hubble Telescope did only slightly better (Weaver et al. 2007) (Figure 4) than the four ground-based astronomers (Haas 1950), indicating the need to get much closer with space probes or build much bigger telescopes (Arnett 2009). For Ganymede, as we shall see, direct exploration proved superior.

Let us jump to 1979, when Frieden and Swindell (1976) carried out what they thought was the first maximum entropy restoration or deconvolution with the positivity constraint,[2] using the two images of Ganymede obtained in 1973 by the Pioneer 10 spacecraft during its trip to Jupiter. But image restoration cannot always make up for inadequate instrumentation: "worse, the artifacts were systematic—that is, highly correlated—and hence indistinguishable from true detail" (Frieden and Swindell 1976: 1237). They had the equivalent of about 140 pixels to work with, so we might roughly say that for all this technology and the passage of time,

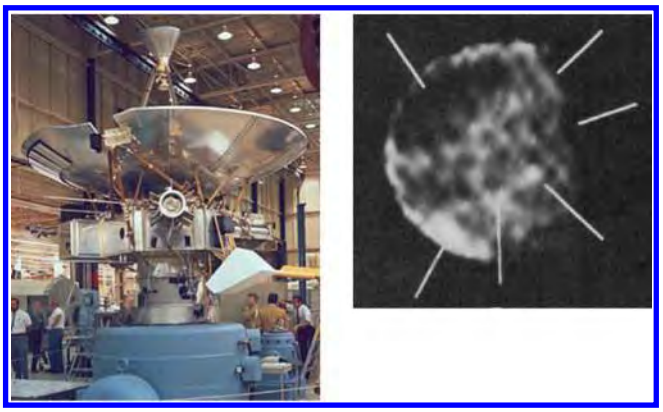

Figure 5.
The Pioneer 10 spacecraft (Minkel 2008; NASA/courtesy of nasaimages.org) and its image of Ganymede restored by a maximum entropy method that includes the positivity constraint (Frieden and Swindell 1976; permission purchased). There is an obvious repetitive artifact through which "features" were marked. Its equatorial diameter is 5,262 km. Resolution is about 400 km (Fimmel et al. 1980).

Figure 6.
Voyager 2 spacecraft (Brandt 2008) and Ganymede as photographed by Voyager 2 in 1979 (Appleton 2008).

the improvement over Galileo's instrumentation (itself "a modest 30-fold improvement in human vision"; Hockey 1999: 18) was an order of magnitude ($\sqrt{140} = \times 12$; Figure 5), showing only "tantalizing markings" (Fimmel et al. 1980). "To my mind . . . the entropy-enhanced pictures [showed] the unexpected presence of very large dark areas, called 'mares'. If you compare today's best pictures of Ganymede with ours it is apparent that these mares were indeed real features, not artifacts" (B. Roy Frieden, personal communication).

However, things were to change fast, as digital cameras and spacecraft improved. The Voyager 2 spacecraft sent back a remarkably improved image of Ganymede (Figure 6), in which we can comfortably distinguish features that could not be confused with artifacts of the imaging system. A new world was opened up to our vision.

It is instructive to take this one more step, to the Galileo Orbiter Spacecraft of 1996 (Figure 7). The improvement in imaging now allowed us to begin defining the geography of the surface (Figures 8 and 9) and begin to visualize Ganymede's three-dimensional (3D) terrain (Figure 10). The excitement of discovery was palpable: "The pictures 'exceeded our wildest expectations'. . . This giant moon was now revealed close-up

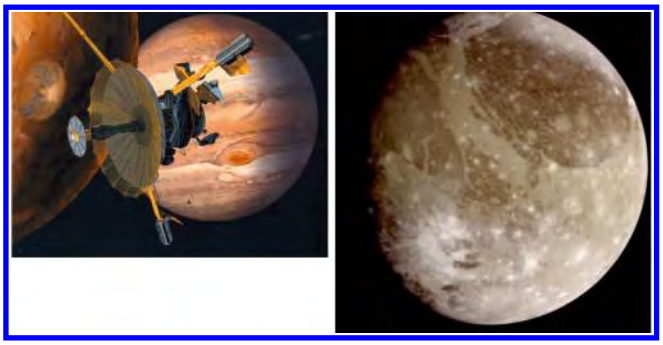

Figure 7.
The Galileo Orbiter spacecraft (Plassmann 2008) and Jupiter's satellite Ganymede as imaged by it in 1996 (Bell II 2003).

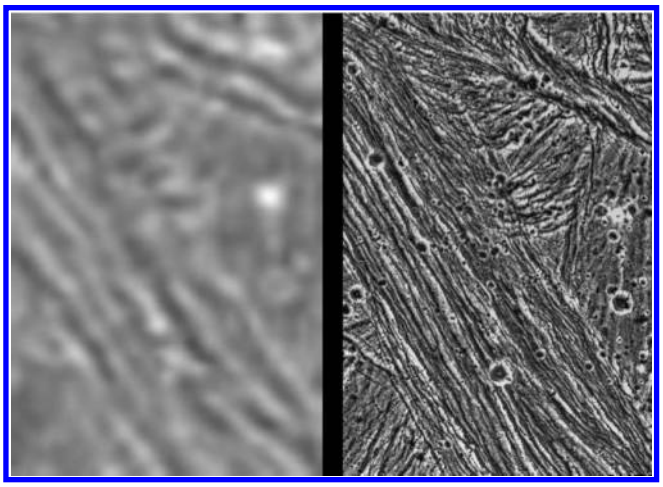

Figure 8.
Comparison of the same region of Ganymede as seen by the Voyager 2 spacecraft in 1979 and the Galileo Orbiter spacecraft in 1996 (Bell II 2003).

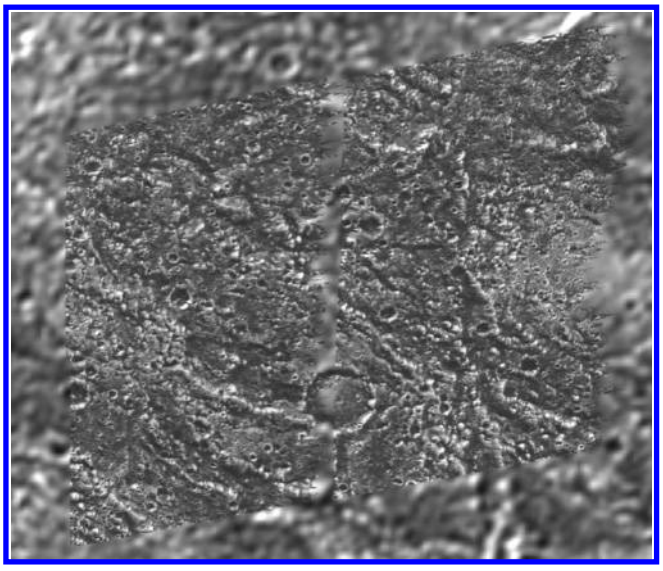

Figure 9.
A montage of new surrounded by old imaging of Ganymede, comparing photos by the Galileo Orbiter spacecraft (center) with the Voyager 2 spacecraft (surround), taken in 1996 and 1979, respectively (Bell II 2003).

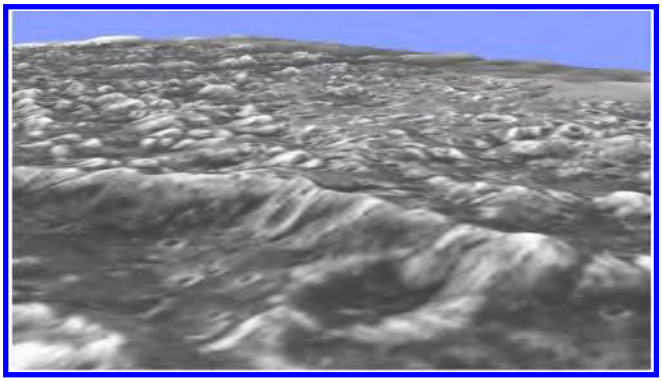

Figure 10.
3D topography of part of Ganymede (Bell II 2003).

for the first time" (Hanlon 2001: 168) (cf. Morrison and Samz 1980; Morrison and Matthews 1982; Fischer 2001).

The exploration of Ganymede continues, with a search for a subsurface ocean and hints of life using the New Horizons spacecraft with infrared spectral imaging (Grundy et al. 2007). I could have picked another moon of Jupiter, such as Io, with over 400 active volcanoes (Lopes et al. 2004), which would now add the dimension of time to our need to observe, or Europa or Callisto, each suspected to also have an ice-covered global ocean.

Lessons for Embryology

One might think, because embryos are so much more accessible than Jupiter's moons, that the problems of imaging them would have been tackled long ago. But the explosion of new microscopy techniques just began in the 1980s, after a lull during which one could just about count the laboratories developing new microscopes on one hand (Mason and Green 1975; Salmon and Ellis 1976; Cremer and Cremer 1978; Willingham and Pastan 1978; Shack et al. 1979; Allen and Allen 1981; Inoué 1981). The problems are a bit different. Ganymede required getting close enough, whereas for embryos we have to overcome field of view and depth of focus versus resolution tradeoffs. Most microscopes are designed for thin slices of dead specimens, so hands-off imaging of ever changing, live, 3D embryos that orient themselves with respect to gravity remains a challenge. This will be taken up in the companion paper (Gordon 2009).

Appendix

Pre-Pioneer Maps and Drawings of Surface Features on Ganymede

http://www.mitpressjournals.org/doi/suppl/10.1162/BIOT_a_00011-Gordon

John E. Westfall
Assistant Jupiter Coordinator, Galilean Satellites
Association of Lunar and Planetary Observers
Antioch CA 94531-2447 USA
johnwestfall@comcast.net

Acknowledgments

I would like to thank Fred Bookstein for extending an invitation to attend the 19th Altenberg Workshop in Theoretical Biology on "Measuring Biology" in 2008, William R. Buckley for a critical reading, and Susan Crawford-Young (Red River College), Stephen P. McGrew (New Light Industries, Spokane), and Ian Paul and Rick Howard (Medical Devices, CancerCare Manitoba) for past and recent discussions. Supported in part by CancerCare Manitoba, Manitoba Institute of Child Health, the Canadian Space Agency, and New Light Industries.

Notes

1. Charles Darwin to Henry Fawcett, September 18, 1861: "How profoundly ignorant B. must be of the very soul of observation! About thirty years ago there was much talk that geologists ought only to observe and not theorize; and I well remember someone saying that at this rate a man might as well go into a gravel-pit and count the pebbles and describe the colours. How odd it is that anyone should not see that all observation must be for or against some view if it is to be of any service!" (Darwin and Seward 1903: 195).

2. Deconvolution methods were developed independently in spectroscopy (Jansson 1984, 1997) and computed tomography, all of which is deconvolution, with a mathematical history stemming from the invention of integral equations by Niels Henrik Abel in 1823, generalized in 1917 by Johann Radon (Radon 1917; Houzel 2004). The ART algorithm, which included the positivity constraint (Gordon et al. 1970), and in unconstrained form is due originally to Kaczmarz (1937), was first applied to reconstruction from electron microscope projections of ribosomes (Bender et al. 1970) and zeugmatography (Lauterbur 1973), now called magnetic resonance imaging (MRI). The first application of deconvolution to light microscopy was in 1977 (Gordon 1983; cf. Agard and Sedat 1983; Shaw 1994).

References

Agard DA, Sedat JW (1983) Three-dimensional architecture of a polytene nucleus. Nature 302: 676–681.

Allen RD, Allen NS (1981) Videomicroscopy in the study of protoplasmic streaming and cell movement. Protoplasma 109: 209–216.

Appleton J (2008) Orwell Astronomical Society (Ipswich). http://www.ast.cam.ac.uk/~ipswich/Miscellaneous/Intro_to_Solar_System/Ganymede.bmp

Arnett B (2009) The World's Largest Optical Telescopes. http://astro.nineplanets.org/bigeyes.html

Bell II EV (2003) NSSDC Photo Gallery: Ganymede. http://nssdc.gsfc.nasa.gov/photo_gallery/photogallery-ganymede.html

Bender R, Bellman SH, Gordon R (1970) ART and the ribosome: A preliminary report on the three-dimensional structure of individual ribosomes determined by an Algebraic Reconstruction Technique. Journal of Theoretical Biology 29: 483–488.

Birks JB (1963) Rutherford at Manchester. New York: Benjamin.

Björklund NK, Gordon R (2006) A hypothesis linking low folate intake to neural tube defects due to failure of post–translation methylations of the cytoskeleton. International Journal of Developmental Biology 50: 135–141.

Brandt WN (2008) Voyager. http://www.astro.psu.edu/users/niel/astro1/slideshows/class39/002-voyager.jpg

Brown MC (2006) Hacking Google Maps and Google Earth. New York: Wiley.

Cremer C, Cremer T (1978) Considerations on a laser-scanning-microscope with high resolution and depth of field. Microscopica Acta 81: 31–44.

Crowder DA (2007) Google Earth for Dummies. Hoboken, NJ: Wiley.

Darwin F, Seward AC, eds (1903) More Letters of Charles Darwin: A Record of His Work in a Series of Hitherto Unpublished Letters. Whitefish, MT: Kessinger Publishing, 2005 Reprint.

Drake S, Galilei G (1957) Discoveries and Opinions of Galileo [Siderius Nuncius]. Garden City, NY: Doubleday.

Encyclopedia Britannica (2009) Two of Galileo's first telescopes; in the Institute and Museum of the History of Science, Florence. Scala/Art Resource, New York. http://media-2.web.britannica.com/eb-media/52/752-004-6FE60E05.jpg

Evans C, Smith RS (2007) Future of Google Earth. Campbell, CA: Madison Publishing.

Fimmel RO, Van Allen JA, Burgess E (1980) Pioneer, First to Jupiter, Saturn, and Beyond. Washington, DC, Scientific and Technical Information Office, National Aeronautics and Space Administration.

Fischer D (2001) Mission Jupiter: The Spectacular Journey of the Galileo Spacecraft. New York: Copernicus Books.

Frieden BR, Swindell W (1976) Restored pictures of Ganymede, moon of Jupiter. Science 191: 1237–1241.

Gordon R (1978) Reconstruction from projections in medicine and astronomy. In: Image Formation from Coherence Functions in Astronomy (Van Schoonveld C, Holland D, eds), 317–325. Dordrecht: Reidel.

Gordon R (1983) Computational embryology of the vertebrate nervous system. In: Computing in Biological Science (Geisow M, Barrett A, eds), 23–70. Amsterdam: Elsevier/North–Holland.

Gordon R (1985) A review of the theories of vertebrate neurulation and their relationship to the mechanics of neural tube birth defects. Journal of Embryology and Experimental Morphology 89 (Suppl.): 229–255.

Gordon R (1999) The Hierarchical Genome and Differentiation Waves: Novel Unification of Development, Genetics and Evolution. Singapore: World Scientific; London: Imperial College Press.

Gordon R (2009) Google Embryo for building quantitative understanding of an embryo as it builds itself. II. Progress toward an embryo surface microscope. Biological Theory 4: 396–412.

Gordon R, Bender R, Herman GT (1970) Algebraic reconstruction techniques (ART) for three-dimensional electron microscopy and x-ray photography. Journal of Theoretical Biology 29: 471–481.

Gordon R, Hoover RB (2007) Could there have been a single origin of life in a big bang universe? Proceedings of SPIE 6694, doi: 10.1117/1112.737041

Gordon R, Hoover RB, Tuszynski JA, de Luis J, Camp PJ, Tiffany MA, Nagy SS, Fayek M, Lopez PJ, Lerner BE (2007) Diatoms in space: Testing prospects for reliable diatom nanotechnology in microgravity. Proceedings of SPIE 6694, doi: 10.1117/1112.737051

Gordon R, Sinnott RW (1983) A cyclopean telescope. Sky and Telescope 65/66: 355.

Griffith Observatory (2009) Zeiss Telescope. http://www.griffithobservatory.org/buildingfiles/buildingimages/bzeiss_telescope.jpg

Grundy WM, Buratti BJ, Cheng AF, Emery JP, Lunsford A, McKinnon WB, Moore JM, Newman SF, Olkin CB, Reuter DC, Schenk PM, Spencer JR, Stern SA, Throop HB, Weaver HA (2007) New Horizons mapping of Europa and Ganymede. Science 318: 234–237.

Haas WH (1950) Four independent simultaneous drawings of Ganymede. Sky and Telescope 9(January): 50.

Hanlon M (2001) The Worlds of Galileo: The Inside Story of NASA's Mission to Jupiter. New York: St. Martin's Press.

Hockey TA (1999) Galileo's Planet: Observing Jupiter Before Photography. Bristol, PA: Institute of Physics Publishing.

Houzel C (2004) The Work of Niels Henrik Abel. New York: Springer.

Inoué S (1981) Video image processing greatly enhances contrast, quality, and speed in polarization-based microscopy. Journal of Cell Biology 89: 346–356.

Jacobson AG, Gordon R (1976) Changes in the shape of the developing vertebrate nervous system analyzed experimentally, mathematically and by computer simulation. Journal of Experimental Zoology 197: 191–246.

Jansson PA (1984) Deconvolution, with Applications in Spectroscopy. Orlando, FL: Academic Press.

Jansson PA, ed (1997) Deconvolution of Images and Spectra. New York: Academic Press.

Kaczmarz S (1937) Angenäherte Auflösung von Systemen linearer Gleichungen. Bulletin international de l'Académie polonaise des Sciences et des Lettres A: 335–357.

Kennedy KH (2009) Introduction to 3D Data: Modeling with ArcGIS 3D Analyst and Google Earth. Hoboken, NJ: Wiley.

Knowledgerush.com (2003) Galileo Galilei. http://knowledgerush.com/kr/encyclopedia/Galileo_Galilei/

Kruschandl NJ (2006) Galileo Galilei 1564–1642. http://www.solarnavigator.net/inventors/galileo_galilei.htm, accessed March 30, 2009.

Lauterbur PC (1973) Image formation by induced interactions: Examples employing nuclear magnetic resonance. Nature 242: 191–192.

Lee H, Bush KT, Nagele RG (1988) Time-lapse photographic study of neural tube closure defects caused by xylocaine in the chick. Teratology 37: 263–269.

Lopes RMC, Kamp LW, Smythe WD, Mouginis–Mark P, Kargel J, Radebaugh J, Turtle EP, Perry J, Williams DA, Carlson RW, Douté S (2004) Lava lakes on Io: Observations of Io's volcanic activity from Galileo NIMS during the 2001 fly-bys. Icarus 169: 140–174.

Mason DC, Green DK (1975) Automatic focusing of a computer-controlled microscope. IEEE Transactions on Biomedical Engineering 22: 312–317.

Minkel JR (2008) Scientists reconstruct the Pioneer spacecraft anomaly. http://www.sciam.com/article.cfm?id=scientists-reconstruct-the-pioneer-spacecraft-anomaly

Morrison D, Samz J (1980) Voyage to Jupiter. Washington, DC, Scientific and Technical Information Branch, National Aeronautics and Space Administration (NASA).

Morrison D, Matthews MS, eds (1982) Satellites of Jupiter. Tucson: University of Arizona Press.

NASA (2009) Hubble's Data Pipeline. http://hubblesite.org/the_telescope/hubble_essentials/image.php?image=pipeline

Plassmann J (2008) The Galileo Spacecraft. http://pirlwww.lpl.arizona.edu/~joep/Work/gll_interlaced.gif

Radon J (1917) Über die Bestimmung von Funktionen durch ihre Integralwerte längs gewisser Mannigfaltigkeiten [On the determination of functions from their integrals along certain manifolds]. Berichte der Sächsischen Akademie der Wissenschaften zu Leipzig, Mathematisch-Physikalische Klasse 69: 262–277.

Rickey DW, Gordon R (2004) Unitron 60 mm Refractor. http://www.cloudynights.com/item.php?item_id=243

Robison WL (1974) Galileo on moons of Jupiter. Annals of Science 31: 165–169.

Salmon ED, Ellis GW (1976) Compensator transducer increases ease, accuracy, and rapidity of measuring changes in specimen birefringence with polarization microscopy. Journal of Microscopy 106: 63–69.

Shack R, Baker R, Buchroeder R, Hillman D, Shoemaker R, Bartels PH (1979) Ultrafast laser scanner microscope. Journal of Histochemistry and Cytochemistry 27: 153–159.

Shaw P (1994) Deconvolution in 3-D optical microscopy. Histochemical Journal 26: 687–694.

Shope R, Fisher D (1999) How astronomers "de-twinkle" the stars. Technology Teacher 59(3): 29–34.

Weaver D, Villard R, Karkoschka E (2007) Hubble catches Jupiter's largest moon going to the 'dark side': HST/WFPC2 image of Jupiter and Ganymede taken April 9, 2007. http://hubblesite.org/newscenter/archive/releases/2008/42/image/a/, http://imgsrc.hubblesite.org/hu/db/images/hs-2008-42-a-full_tif.tif

Willingham MC, Pastan I (1978) The visualization of fluorescent proteins in living cells by video intensification microscopy (VIM). Cell 13: 501–507.

Supplement to: (Gordon & Westfall, 2009)

Appendix

Pre-Pioneer Maps and Drawings of Surface Features on Ganymede

(In chronological order of publication. Compiled by J. Westfall, Feb. 26, 2009)

These references are limited to books and articles either in my personal collection or available online, or to works referred to in those references. I have included only those works that directly refer to, or show drawings of, surface markings on Ganymede, earlier than the first space-probe image of Ganymede (acquired by Pioneer 10 on December 3, 1973). The only earlier photographs that I know of that show Ganymede's surface markings are the red-blue pair taken by the Palomar Observatory 200-inch on October 24, 1952 (there may well be others taken prior to Pioneer 10; nowadays earth based amateurs and professionals, along with the HST, almost routinely record surface detail on Ganymede). Except for the William Herschel item, I have not included references on light variations, elliptical appearances or "dark transits," which all imply surface markings.

Walter H. Haas (personal communication) notes: "Since we have been able to make maps of Ganymede in recent years, we can now know what features on its surface were actually turned toward the Earth at the time of old observations of surface markings". This would allow us to know, in retrospect, whether any of these observations, were more than mental constructs, such as those that led to the idea of Martian made canals on Mars (Markley, 2005).

Herschel, William (1797). "Observations of the Changeable Brightness of the Satellites of Jupiter, and of the Variation in their Apparent magnitudes; with a Determination of the Time of their Rotary Motions on their Axes. To which is Added, a Measure of the Diameter of the Second Satellite, and an Estimate of the Comparative Size of all the Four." *Philosophical Transactions, Royal Society*, 87: 332-351. [Herschel suggests that the satellites are "variegated" and rotate, explaining their brightness changes. (p. 344).]

Schroeter, Johann Hieronymus (1800-1801). *Astronomisches Jahrbuch*, 1800: 169-170; 1801: 126. [Schroeter observed a dark marking on Ganymede on 3 nights in 1796. Referred to by Schaeberle and Campbell (1891), p. 359.]

Dawes, William Rutter (1860). "On the Appearance of Jupiter's Satellites while Transiting the Disk of the Planet." *Monthly Notices, Royal Astronomical Society*, 20: 245-247. [2 drawings of Ganymede made in 1849 and 1860 on Pl. 2, f. p. 244. The 1849 drawing is the earliest found to date.]

Guillemin, Amédée (1877). *Le Ciel. Notions Élémentaires d'Astronomie Physique*. Paris: Librairie Hachette et Cie. [6 drawings of Ganymede by Secchi in 1855, p. 471.]

Chambers, George Frederick (1889). *A Handbook of Descriptive and Practical Astronomy*. 4th ed. Oxford: Clarendon Press. [Drawings of Ganymede by Secchi on Vol. 1 title page, and by Dawes on Vol. 1 p. 189]

Holden, Edward S. and Campbell, William Wallace(1891). "Observations of Jupiter and of his Satellites with the 36-inch Equatorial of the Lick Observatory (1888-1890)." *Publications, Astronomical Society of the Pacific*, 3: 265-272. [Description of dark markings on Ganymede, p. 272.]

Schaeberle, John Martin and Campbell, William Wallace (1891). "Observations of Markings of Jupiter's Third Satellite." *Publications, Astronomical Society of the Pacific*, 3: 359-365. [12 drawings of Ganymede by the authors f. p. 359.]

Proctor, Richard Anthony; completed by Ranyard, A. Cowper (1892). *Old and New Astronomy*. London: Longmans, Green, and Co. [2 drawings by Dawes in 1860 and 1845 (Fig. 397) and 4 by Secchi in 1855 (Fig. 398), p. 602.]

Douglass, Andrew Ellicott (1897). "Drawings of Jupiter's Third Satellite." *Astronomisches Nachrichten*, 143: 411-414. [27 drawings and map of Ganymede f. p. 412.]

Barnard, Edward Emerson (1897). "On the Third and Fourth Satellites of Jupiter." *Astronomisches Nachrichten*, 144: 321-330. [16 drawings of Ganymede on plate.]

Molesworth, Percy Braybrooke (1899). "Satellite Observations and Studies." *Memoirs, British Astronomical Association*, 7: 207-210. [Within Jupiter Section report.]

Phillips, Theodore Evelyn Reece (1906). "Eleventh Report of the Jupiter Section." *Memoirs, British Astronomical Association*, 14 (III): 92-93.

Innes, Robert Thornton Ayton (1909). "Observations of Jupiter's Galilean Satellites, January-June, 1908." *Monthly Notices, Royal Astronomical Society*, 69: 512-538. [18 drawings of Ganymede on Pl. 20; comments on pp. 535-538.]

Phillips, Theodore Evelyn Reece (1911). "Fifteenth Report of the Section for the Observation of Jupiter." *Memoirs, British Astronomical Association*, 17 (IV):113-134. [3 drawings of Ganymede on Pl. IV, Fig. 2.]

Phillips, Theodore Evelyn Reece (1913). "Sixteenth Report of the Section for the Observation of Jupiter." *Memoirs, British Astronomical Association*, 19 (III): 59-71. [4 drawings of Ganymede on Pl. IV, Figs. 5-8; notes on pp. 69-71.]

Steavenson, William Herbert (1915). "Ganymede." *Journal, British Astronomical Association*, 25: 383-385.

Phillips, Theodore Evelyn Reece and Steavenson, W. H. (1917). "A Remarkable Transit of Jupiter's Third Satellite." *Journal, British Astronomical Association*, 28: 56-59.

Webb, Thomas William (1917/1962). *Celestial Objects for Common Telescopes*. New York: Dover Publications. [Dover reprint of 6th edition, 1917. Drawings of Ganymede by Burton in 1860 and 1849 and by Secchi in 1855, on pp. 200-201.]

Berget, Alphonse (1923). *Le Ciel*. Paris: Librairie Larousse. [2 drawings of Ganymede by E. E. Barnard on p. 118.]

Phillips, Theodore Evelyn Reece and Steavenson, William Herbert, eds. (1925). *Splendour of the Heavens*. New York: Robert M. McBride &Company. [2 drawings of Ganymede in 1917 in Vol. 1, p. 356.]

Phillips, Theodore Evelyn Reece (1927). "Twenty-third Report of the Jupiter Section." *Memoirs, British Astronomical Association*, 27 (IV): 87-88.

Anon. (1932). *Memoirs, British Astronomical Association*, 34 (2): Pl. XII. [Drawing of Ganymede by W. H. Steavenson on Feb. 18, 1932.]

Antoniadi, Eugene Michel (1939). "On the Markings of the Satellites of Jupiter in Transit." *Journal, Royal Astronomical Society of Canada*, 33: 273-282. [Drawing of Ganymede by author on Pl. XI (f. p. 273), with comments on pp. 277-278.]

Lyot, Bernard (1943). "Observations Planétaires au Pic du Midi en 1941 par MM. Camichel, Gentili et Lyot." *Bulletin, Société Astronomique de France (L'Astronomie)*, 57: 49-60, 67-72.

Camichel, Henri; Gentili, Marcel and Lyot, Bernard (1944). "Observations Planetaires au Pic du Midi en 1941." *Ciel et Terre*, 60: 135-137. [Note on Ganymede on p. 137.]

Danjon, Andre (1944). :"Les Satellites de Jupiter." *Bulletin, Société Astronomique de France (L'Astronomie)*, 58: 33-36.

Lyot, Bernard (1945). “Planetary and Solar Observations on the Pic du Midi in 1941, 1942, and 1943.” *Astrophysical Journal*, 101: 255-259, Pl. XIX-XXV. [Note on p. 258.]

Haas, Walter H. (1950). “Four Independent Simultaneous Drawings of Ganymede.” *Sky and Telescope*, 9 (Jan.): 50. [Reprinted with illustration in: Corliss, William R., ed. (1979). *Mysterious Universe: A Handbook of Astronomical Anomalies*. Glen Arm, MD: Sourcebook Project. pp. 447-448.]

Cave, Thomas R., Jr. (1951). “Fig. 6. Jupiter III. T. R. Cave, Jr. 36-inch refr. Aug. 17, 1950 7h 20m, U.T. 740X.” *The Strolling Astronomer [J.A.L.P.O.]*, 5 (3, March 1): 1 (Figure 6). [Drawing; see also: Hare, Edwin E., “Jupiter 1950 report No. 4”, pp. 8-10 in the same issue.]

Reese, Elmer J. (1951). “Map of Ganymede in 1949. Drawing by E. J. Reese.” *The Strolling Astronomer [J.A.L.P.O.]*, 5 (7; July 1): 1 (Figure 1). [See also “Observations and Comments,” pp. 9-10.]

Both, Ernst E. (1952). “Jupiter’s Satellite Ganymede in 1951-52.” *The Strolling Astronomer [J.A.L.P.O.]*, 6 (6; June 1): 78-81. [Map of Ganymede by T.E. Howe on p. 79.]

Lyot, Bernard (1953). “L’Aspect des Planetes au Pic du Midi dans une Lunette de 60 cm d’Ouverture.” *Bulletin, Société Astronomique de France (L’Astronomie)*, 67:3-21. [47 drawings on p. 18; map on p. 20.]

Avigliano, D. P. (1954). “Jupiter’s Satellites, 1953-54.” *The Strolling Astronomer [J.A.L.P.O.]*, 8: 11-14. [Map of Ganymede on p. 12.]

Brookes, Robert G. (1954). “Jupiter in 1953-54: Interim Report.” *The Strolling Astronomer [J.A.L.P.O.]*, 8: 118-122. [Drawings of Ganymede on pp. 119-120.]

Squyres, Henry P. (1957). “Jupiter in 1956-57: First Interim Report.” *The Strolling Astronomer [J.A.L.P.O.]*, 11: 15-20. [Drawings of Ganymede on p. 17, notes on p. 18.]

Reese, Elmer J. (1959). “The 1957-58 Apparition of Jupiter.” *The Strolling Astronomer [J.A.L.P.O.]*, 13: 58-81. [Drawing of Ganymede on p. 67.]

Rudaux, Lucien and de Vaucouleurs, Gérard Henri (1959). *Larousse Encyclopedia of Astronomy*. New York: Prometheus Press. [3 drawings of Ganymede by Antoniadi and 4 by Lyot, Camichel and Gentili, on p. 217.]

Budine, Phillip W. (1960). “Jupiter in 1959: Second Interim report.” *The Strolling Astronomer [J.A.L.P.O.]*, 14: 34-43. [Drawings of Ganymede on p. 43.]

Dollfus, Audouin (1961). “Visual and Photographic Studies of Planets at the Pic du Midi.” In: Kuiper, Gerard P. and Middlehurst, Barbara M., eds., *Planets and Satellites* (Chicago: University of Chicago Press): Cpt. 15, pp. 534-571. [Ganymede drawings and map on p. 567 and Pl. 40.]

(Haas, Walter H.) (1961). “Observations and Comments.” *The Strolling Astronomer [J.A.L.P.O.]*, 15: 218-220. [Drawings of Ganymede on front cover and p. 219.]

de Callataÿ, Vincent and Dollfus, Audouin (1967). *Atlas of the Planets*. tr. by Collon, Michael. Toronto: University of Toronto Press. [Drawings of Ganymede on pp. 117-118, map on p. 120.]

Roth, Günter D., tr. by Alex Helm (1970). *Handbook for Planet Observers*. London: Faber and Faber. [6 drawings of Ganymede by six different A.L.P.O. observers in 1961, p. 175.]

Dollfus, Audouin and Murray, John B. (1974). “La Rotation, la Cartographie et la Photometrie des Satellites de Jupiter.” In: Woszczyk, A. and Iwaniszewska, C., eds., *IAU Symp. No. 65, Exploration of the Planetary System* (Dordrecht: IAU/Reidel): 513-525. [Drawings of Ganymede on pp. 515, 516 and 521; map on p. 519; albedo map on p. 522.]

Murray, John B. (1975). “New Observations of Surface Markings on Jupiter’s Satellites.” *Icarus*, 25: 397-404. [Albedo map and drawings made by author in 1941 and1973.]

Rogers, John H. (1995). *The Giant Planet Jupiter*. Cambridge: Cambridge University Press. [See “Surface markings,” pp. 324-329; drawings of Ganymede on pp. 325 and 328, map on p. 329.]

References

Gordon, R. & J.E. Westfall (2009). Google Embryo for building quantitative understanding of an embryo as it builds itself: I. Lessons from Ganymede and Google Earth. *Biological Theory: Integrating Development, Evolution, and Cognition* **4**(4), 390-395.

Markley, R. (2005). *Dying Planet: Mars in Science and the Imagination*. Durham, Duke University Press.

Google Embryo for Building Quantitative Understanding of an Embryo As It Builds Itself. II. Progress Toward an Embryo Surface Microscope

Richard Gordon
Department of Radiology
University of Manitoba
Winnipeg, Manitoba, Canada
gordonr@cc.umanitoba.ca

Abstract
Embryos start out as tiny globes, on which many important events occur, including cell divisions, shape changes and changes of neighbors, waves of contraction and expansion, motion of cell sheets, extension of filopodia, shearing of cell connections, and differentiation and morphogenesis of tissues such as skin and brain. I propose to build a robotic microscope that would enable a new way to look at embryos: Google Embryo. This is akin to sending a space probe to Jupiter and its moons, sending back spectacular new visions of their complexity, activity, and beauty.

Keywords
differentiation, embryogenesis, Google Earth, robotic microscopy, stem cells, time-lapse imaging

December 6, 2009; accepted January 6, 2010
Biological Theory 4(4) 2009, 396–412.

In embryology we are in the midst of a similar trend to that of spectacularly improving astronomical instrumentation and imaging (Gordon and Westfall 2009), but are way behind our technological potential: for lack of will (funding); for lack of a desire for quantitation; for believing that all answers lie in molecular and genomic approaches; and for not studying embryo physics (Forgacs and Newman 2005; Beloussov and Gordon 2006; Gordon and Buckley 2010), as if embryos are not part of the physical world. Let us think of the ultimate goal of quantitation of embryogenesis in the following way. While we generally identify a species by its adults, in truth all organisms undergo a life cycle, and any stage of that life cycle gives rise to the next (i.e., organisms are at least four dimensional; Gamow 1970; Banchoff 1990; Konijn et al. 1996; Schnabel et al. 1997; Zimmermann and Siegert 1998; Radlanski et al. 1999; Eliceiri et al. 2000; Hammond and Glick 2000; Heid et al. 2002; Salihagic-Kadic et al. 2005; Boot et al. 2008). Thus, there is a certain arbitrariness to where we begin.

Physicists like to keep things simple and are wont to start off "given a spherical cow. . . " (Harte 1988; Doyle 2001; Austin and Chan 2003). Fortunately, cows are indeed spherical at the one-cell fertilized egg stage, prior to the first cell division, and this stage has biological properties suggesting no hidden symmetries beyond the visual spherical symmetry[1] (Evsikov et al. 1994; Gordon 1999; Rivera-Perez 2007; Johnson 2009). So all that a cow is going to be, except perhaps for the things it learns after it develops a brain and immunities, is somehow contained in that tiny sphere. For humans, the diameter is 70 μm (see Figure 1). Thus I choose to begin with the one cell-fertilized embryo.

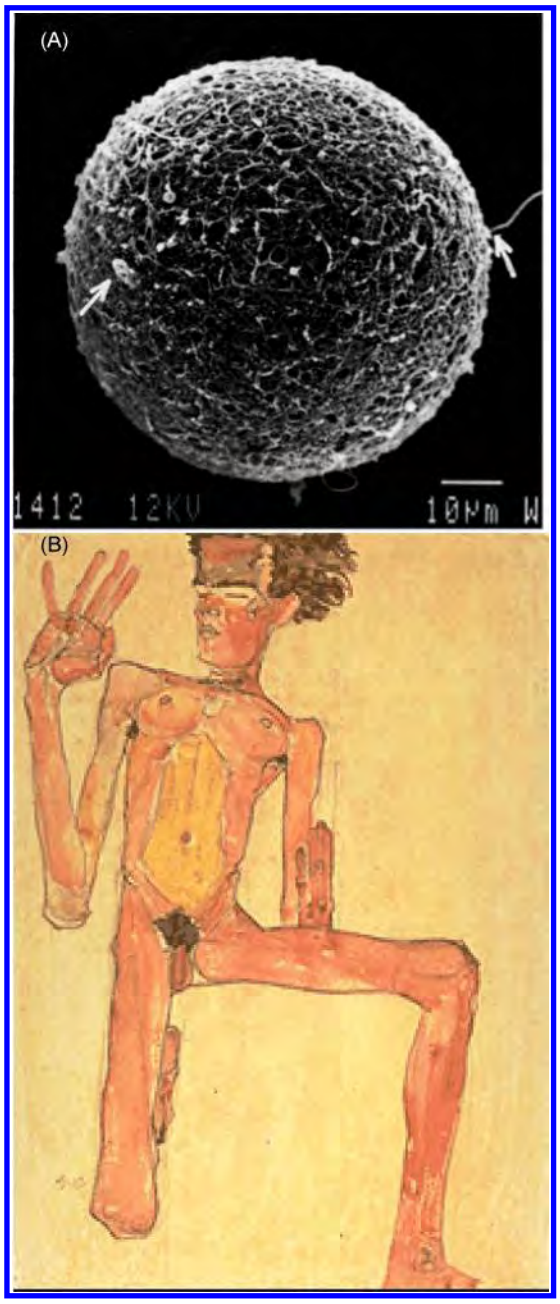

Figure 1.
How did your spherically symmetrical egg turn into a highly asymmetrical shape? We are not even bilaterally symmetric, if you consider the brain, your internal organs, and your left or right handedness! (A) Scanning electron micrograph of sperm attached to a human egg (Nikas et al. 1994), with permission. (B) Egon Schiele's "Kneeling Male Nude," a self-portrait of the Austrian artist made in 1910 (Chan 1997), in public domain.

Imaging the Living Axolotl Embryo

The axolotl embryo starts off as the fertilized egg, Stage 1, with a jelly coat that protects the embryo (see Figures 2 and 3). It is easy to remove, and ordinarily it becomes cloudy after a while, so embryologists remove the jelly for a better view and put the embryo in a dilute, sterilized salt solution to reduce the chance of infection by bacteria or fungi. There is some evidence that removal of the jelly affects development (Mietchen et al. 2005a, b).

At Stage 2 first cleavage has occurred, and the embryo now consists of two large cells called blastomeres, followed by four blastomeres at Stage 3. Next, cleavage occurs at right angles to the previous ones, resulting in eight cells at Stage 4, but notice that the bottom blastomeres are larger. This may be due to the high viscosity of the yolk that is concentrated at the bottom of the embryo, but the actual physics has yet to be investigated.

Stage 5 has 16 cells, the result of more vertical cleavages. Note that the top cells are cleaved off first: cleavage actually occurs in a wave from top to bottom. The synchrony of cell division is lost over Stages 6–9 (Hara 1971; Yoneda et al. 1982; Boterenbrood et al. 1983; Boterenbrood and Narraway 1986; Wang et al. 2000). As the cells are getting smaller and smaller, the artist got tired of drawing them all by Stage 9 (see Figure 3).

At Stage 10, a dimple appears on the surface that acts as if you had pushed your thumb into a soft ball. The inside is actually a hollow above this "dorsal lip of the blastopore"

Figure 2.
Female white mutant axolotl, the salamander *Ambystoma mexicanum*, laying 2-mm-diameter eggs in jelly capsules (Crawford-Young 2007). Used with permission.

called the blastocoele that started forming at the two-cell stage (Fleming et al. 2000). The left and right sides of the embryo are now obvious. But note that they were determined by the major event of cortical rotation that occurs before Stage 2 (Nouri et al. 2008), which is visually subtle and thus not represented by its own stage.

Through Stage 13, half of the outer layer of cells moves inside via the blastopore, which visibly becomes a circle (Stage 12) that then shrinks to a point (Stage 13). The blastopore is actually a wave of contraction moving through the cells, made visible by their pigment granules temporarily squeezed together, that is nearly stationary in the laboratory coordinate system, and thus usually mistaken for an object rather than a process (Gordon 1999).

The upper hemisphere develops a neural ridge at Stage 14 that demarks the neural plate from the epidermis. The neural plate narrows into a keyhole shape, Stage 16, and then seals as a tube at Stage 19. The epidermis has, in the meantime, expanded so that it covers the whole embryo, and, in fact, it even ends up over the neural tube. Later on the epidermis will become the skin of the animal.

The round part of the neural plate at Stage 16 will later become the brain, and the narrow part will become the spinal cord. Thus the neural plate, a layer of cells one cell thick, is the source of the central nervous system (CNS).

Three features of embryonic development are apparent in Stages 19 to 22: the eyes form, the brain segments, and many somites form to the sides of the CNS. The somites give rise to the segmented muscles and ribs of the animal and the vertebrae.

The rest of embryonic development takes the axolotl embryo to the hatching, larval stage. It looks, at Stage 44, pretty much like an adult, except that the four legs have yet to bud and grow out. Now it can eat and increase its dry mass. Presumably, cell size reduction through cell division also ceases.

Note that the sketches in Figure 3, although published in 1989 (Bordzilovskaya et al. 1989), are still hand-drawn.

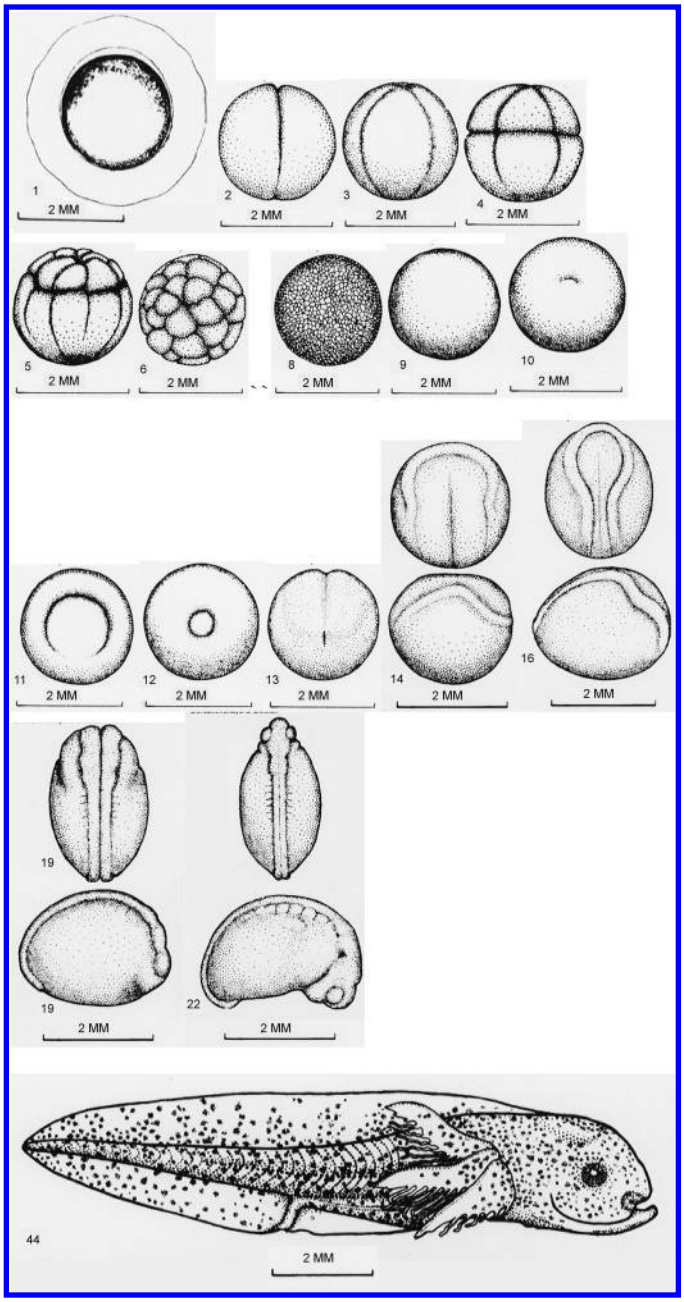

Figure 3.
Staging of axolotl development (Bordzilovskaya and Dettlaff 1979; Bordzilovskaya et al. 1989; with permission of S. Randal Voss, Ambystoma Genetic Stock Center, University of Kentucky). Stages 1–5, 44 are shown in side view, 6–9 in top view, 10–13 in bottom view, 14–22 in top and side views. Stages are based on recognizable morphologies, so that timing between stages is irregular (besides being temperature-dependent). The hatching Stage 44 is reached after 2 weeks at 20°C.

Even the century-old art of photography had not penetrated embryology at that date, at least to the point where it was the preferred visualization approach for the living embryo. (Other papers on staging have used photography (Schreckenberg and Jacobson 1975).) This is perhaps because of depth of focus limitations of all microscopes. The first through-focus mosaic of an embryo, literally made by cutting out the in-focus regions

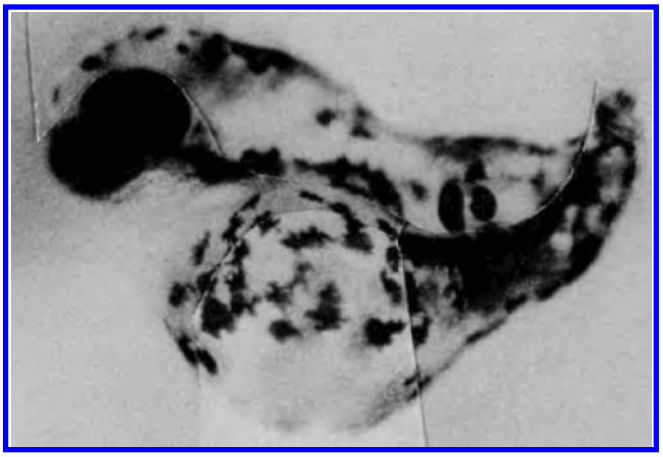

Figure 4.
The first through-focus mosaic of a living embryo (Gordon 1983). Reproduced with permission of Elsevier.

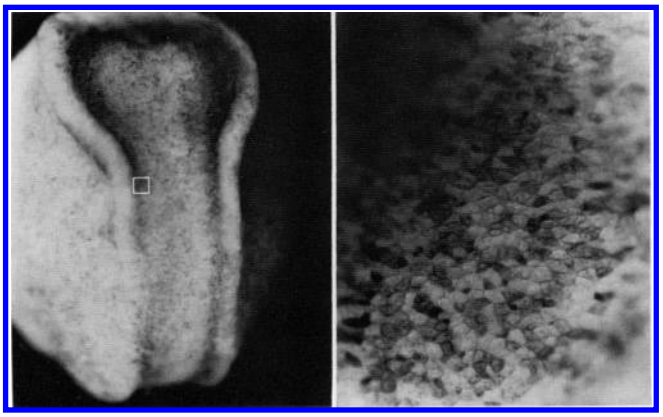

Figure 5.
The highly variegated pigmentation of Urodele amphibian embryos permits tracking of clumps of pigment or single cells (Jacobson and Gordon 1976a with permission). The embryo is 2 mm in diameter and the cells are about 15 μm across at this open neural plate stage during which the brain and spinal cord are being formed (Cf. Jacobson and Gordon 1976b, 1977; Gordon and Jacobson 1978). Reproduced with permission of John Wiley & Sons.

from a through-focus series of images of a tailless zebrafish embryo, is shown in Figure 4. This technique in effect turns the microscope into a telephoto lens. While there is now a large digital image processing literature on the method and much active research (Dowski and Johnson 2002; Forster et al. 2004; Ortyn et al. 2007; Aguet et al. 2008; Caron and Sheng 2008), it is not yet widely used in biology, let alone embryology.

One tremendous advantage of the axolotl and other urodeles is that the cells in the early embryo are highly variegated in pigmentation (see Figure 5). This both marks the shape of each cell and permits easy cell tracking (Burnside and Jacobson 1968; Brodland et al. 1996).

Time-Lapse Imaging of Live Embryos

Time-lapse microscopy of live embryos was a tedious procedure in the predigital era. Film movie cameras had to be modified to take one frame at a time, focus had to be adjusted by hand, and generally images were of low resolution and taken from only one view. Illuminator bulbs would burn out at inopportune times. Images were small, taken usually on 16-mm film. Framing intervals had to be chosen in advance, so that events occurring an order of magnitude faster or slower were missed. The convention of the time seems to have been a 1000 $\times$ speedup. Time markers were generally not available and editing involved cutting and gluing the film. Review of films was done with specialty stop motion movie projectors, aircooled to keep the film from melting, with cells or other events recorded by hand frame by frame from the images projected onto large sheets of paper. It is no wonder that the amphibian time-lapse literature was generated by only a handful of researchers (Hara 1971; Keller 1978, 1981; Yoneda et al. 1982; Boterenbrood et al. 1983; Ubbels et al. 1983; Keller and Spieth 1984; Boterenbrood and Narraway 1986, 1990; Keller and Hardin 1987; Hardin and Keller 1988; Keller and Danilchik 1988; Keller et al. 1989; Wilson and Keller 1991; Niehrs et al. 1993; Wang et al. 2000). Dual imaging of top and bottom of an embryo was a major innovation (Hara 1970), even though the equator was missed, being seen only tangentially. Video time-lapse came in for a while (Ubbels et al. 1983; Keller et al. 1985; Asada-Kubota and Kubota 1991; Keller et al. 1992; Nieuwkoop et al. 1996; Parichy 1996; Elul et al. 1997; Pérez-Mongiovi et al. 1998) and was soon digitized (Fire 1994). In a way this was a step backward because of the reduced resolution compared to film. With the advent of digital cameras, automatic focusing (LeSage and Kron 2002) and 3D imaging during time-lapse became facile (Ewald et al. 2004), and with ever increasing numbers of megapixels per image, digital imaging no longer sacrifices spatial resolution.

Beyond Sketches of the Axolotl Embryo Surface

Because of the yolk and surface pigmentation, axolotl and other amphibian embryos scatter light greatly in their early stages of development and are, in effect, visually opaque. In a way this is a benefit, because before neural tube closure, most of the action is on the surface, and the scattered light provides back lighting of the surface pigment, making the surface cells highly visible. In fact, we have found that albino axolotl embryos, lacking pigment, are almost impossible to stage alive. Thus the next step in live amphibian embryo imaging is to capture the whole pigmented surface at once. Significant changes can occur on the time scale of minutes (Gordon et al. 1994), a fact that requires that the whole surface be imaged rapidly. But first one has to choreograph the geometric gymnastics of imaging the full embryo surface.

The first attempt to image the whole surface of an axolotl embryo was to literally rotate a stereomicroscope bearing a vidicon camera, and its illuminator, around an embryo sitting on a rotating pedestal in a cuvette. The design was inspired by the Landsat satellite that viewed the surface of the Earth

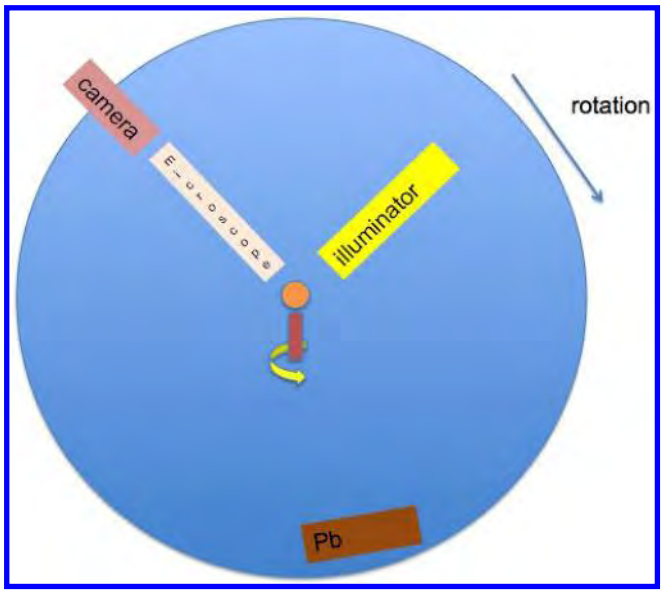

Figure 6.
Landsat approach to surface imaging of an axolotl embryo, in which a stereomicroscope, video camera, and halide illuminator with heat filters are rotated on a 5' (1.5 m) diameter wheel, orbiting around an embryo on a pedestal, in a chamber. The lead (Pb) weights are used to balance the mass (Gordon 1982).

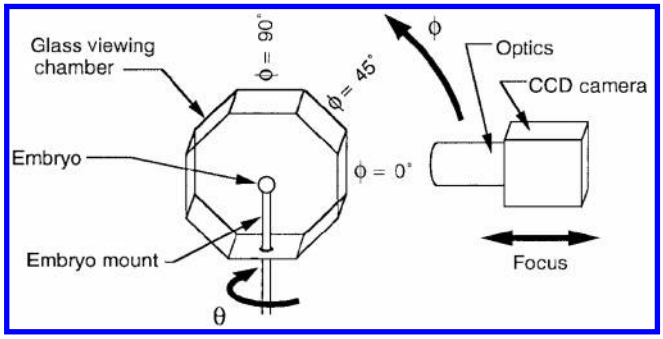

Figure 7.
One approach to imaging most of the surface of an axolotl embryo (Brodland and Veldhuis 1998), with permission of the first author and the publisher.

(Gordon 1982) (Figure 6). (An amusing interlude involved a hollow pedestal tube with a slight negative pressure to keep the embryo from falling off. However, the viscoelastic embryo responded by producing a long "pseudopod" sucked into the tube!) Note that the pedestal obscures the bottom view, so that this design does not quite achieve full 4π solid angle coverage. Recording was onto video home system videotape, as hard disk drives of that era did not have sufficient storage, and the tape drive was digitally driven intermittently as needed by the computer, to minimize tape usage. Unfortunately, the computer driving the stepping motors and tape recorder never worked and had to be replaced, and the attempt was not successful before funding ran out and the team dispersed. A similar, albeit more compact design made possible by CCD cameras, has indeed produced surface mosaic images that can be stitched together (Brodland and Veldhuis 1998) (Figure 7). But the optics used do not allow a fine enough finite element grid to

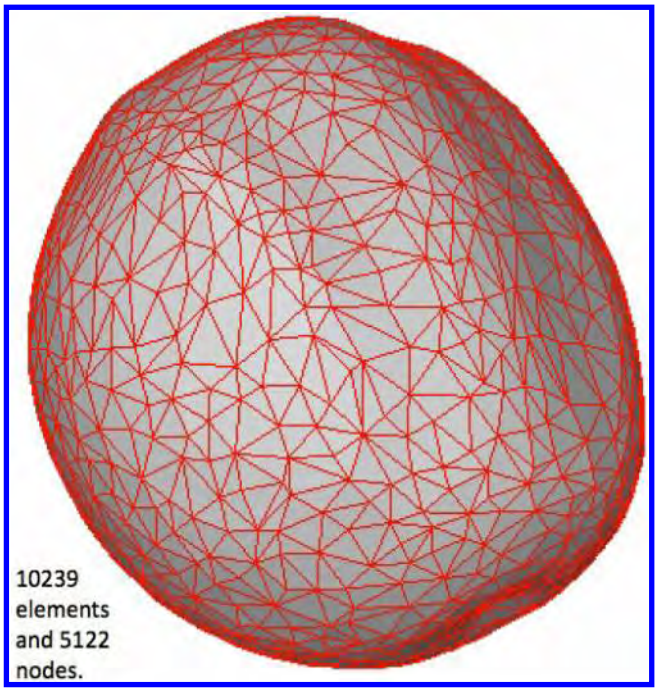

Figure 8.
A finite element grid of 10,239 elements with 5,122 nodes, a mesh still well above cellular level (Chen and Brodland 2008), with permission.

represent the cells (Figure 8), let alone alterations in cell size, shape, and details of pigmentation (Figure 9).

I considered numerous ways to overcome the problem of observing the live embryo as if it were floating in space like Ganymede (Gordon and Westfall 2009), and we could blithely take pictures all around. An embryo could be placed in free fall in water between two sheets of glass, which would move relative to one another, causing it to tumble in the changing shear. Rotation of the sheets would keep it suspended indefinitely. But these embryos are bottom heavy due to the nonuniform distribution of yolk (Nouri et al. 2008), so the angle coverage would be nonuniform, and there would be a difficult image processing job trying to match the snapshots one to the other to form a mosaic or stitched image of the surface. The effect of constant tumbling on early development is unknown, although after neurulation and the development of cilia, axolotl embryos rotate constantly on their own (Twitty 1928).

Another fanciful scheme involved suspension with four nearly vertically directed jets of water, whose slightly different velocities would provide torque for tumbling. This was inspired by the trick of suspending a ball in the stream of a vertically directed water hose.

Six cameras aimed at six overlapping hemispheres might work, except that with microscope objectives of normal working distances, the objectives would physically overlap, making this design impossible. A tetrahedral arrangement would alleviate the steric restriction a bit.

These thoughts finally led to a workable design, using tiny prisms slightly larger than the embryo (Figure 10). The

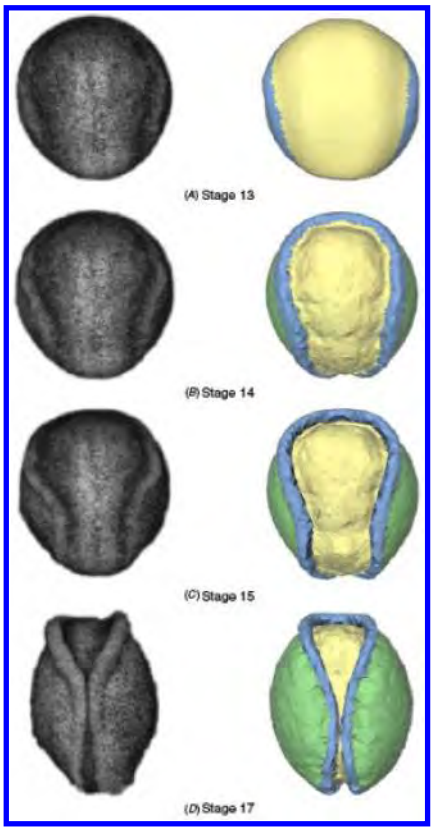

Figure 9.
Micrographs and rendered surface images of axolotl embryos during neurulation (Chen and Brodland 2008), with permission. Note that despite the fine mesh of 10^4 elements, the number of cells is at least 4×10^4, so that cells are not represented, let alone portrayed in any detail.

six views were thus obtained as: one directly down, to a stereomicroscope (which has a long working distance); four down via the right angle prisms; and one up through a 4 × water immersion objective. The latter was built into a homemade microscope in which the objective projected an image of the full width of the embryo onto a CCD camera chip without any intervening optics. The design grew as problems were solved, into a Rube Goldberg-like (Wolfe and Goldberg 2000) device (Figure 11).

One problem encountered was that the prisms blocked the light, creating nonuniform illumination of the embryo's surface. This was alleviated using fiber optics attached to the top objective (Figure 12), a ring light (Figure 13), and fiber optic threads placed right through the prism holder (Figure 14). The lighting was still nonuniform, but this was partly compensated by histogram equalization (Russ 2002) (Figure 15).

As can be seen from Figure 16, vertical focusing is required not only for the through-focus mosaic but also because, with the longer optical path length (i.e., integral of distance times refractive index) through the prisms, the central image has a different focal plane from the four side views. Problems with keeping the optical pathway clean are also apparent.

Of course, the depth of focus of the objectives was less than the 1-mm depth of the hemisphere observed, so a few through focus mosaic techniques were implemented and compared (Crawford-Young 2007).

The next step, yet to be achieved, is to project the images of the embryos onto a virtual sphere, which is a good approximation to the shape of the embryo through Stage 13. Each point on the sphere would "see" three of the images, so the corresponding pixels in the three through focus mosaic images were weighted by the squares of their direction cosines, measured relative to the normal to the surface voxel of the sphere whose value was being assigned (Figure 17).

We now have cellular resolution, but just (Figure 18). As each cell is about 15-μm wide, at a limiting resolution for light microscopy, we could profitably, by the Nyquist criterion, use a pixel grid of 60 × 60 pixels for a cell (0.25 μm). Pixels here are 1.2-μm wide.

Problems with the prototype robotic microscope include the following:

- Nonuniform illumination.
- The water immersion objective moves the embryo via its contact with the surrounding jelly (which is used to keep the embryo centered and protected from infection by bacteria and fungi).
- It is difficult to clean the optical paths, since dirt can get between the coverslip and the prisms.
- Our choice to use optics that image the full width of the embryo restricts spatial resolution.
- The camera speed restricted the framing rate to one full cycle of images (say 3 focal planes per view × 6 views = 18 images per time step) every 5 minutes.
- Components were added as problems became apparent, and so overall design is suboptimal.
- The algorithm for creating a surface rendition of the embryo is restricted to the early spherical shape, and deviations from sphericity are not taken into account.

New Approach to Axolotl Robotic Microscopy

Most light microscopes do not have zoom capabilities, and a mental constraint on the first robotic microscope (Crawford-Young 2007) was that it should be able to image a whole hemisphere at once. Part of the difficulty was the need for at least 1-mm working distance, which is the distance from the lens to the object being imaged, i.e., the radius of the embryo. In general, there has been a tradeoff between working distance and magnification for biological microscope objectives. My first thought on this, in the early 1970s while visiting the laboratory of Antone G. Jacobson (Jacobson and Gordon 1976a, b; Gordon and Jacobson 1978; Jacobson 1980) was to use a Questar telescope. Indeed, the company came out with a series of

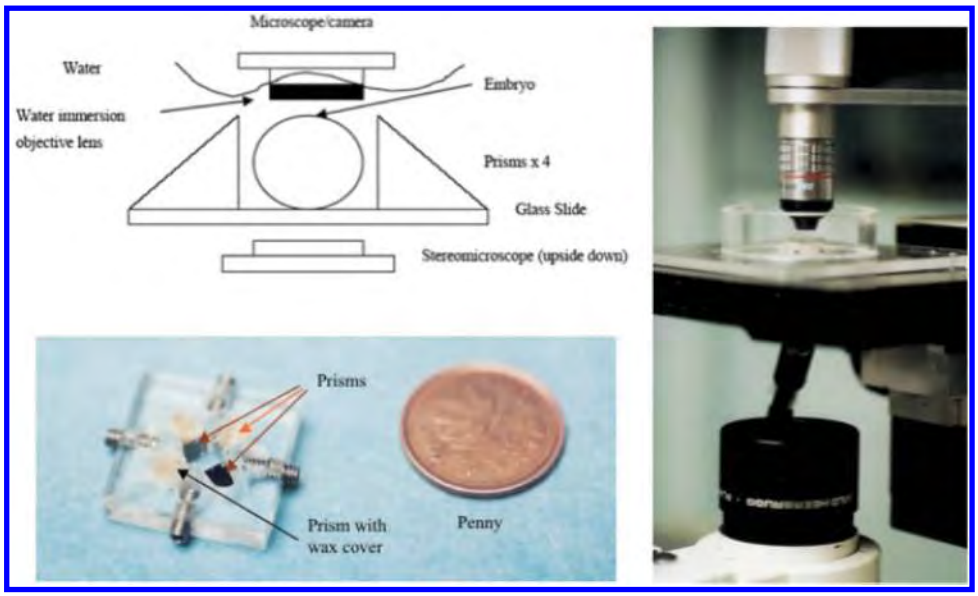

Figure 10.
Construction of the robotic microscope for single axolotl embryos (Crawford-Young 2007), with permission.

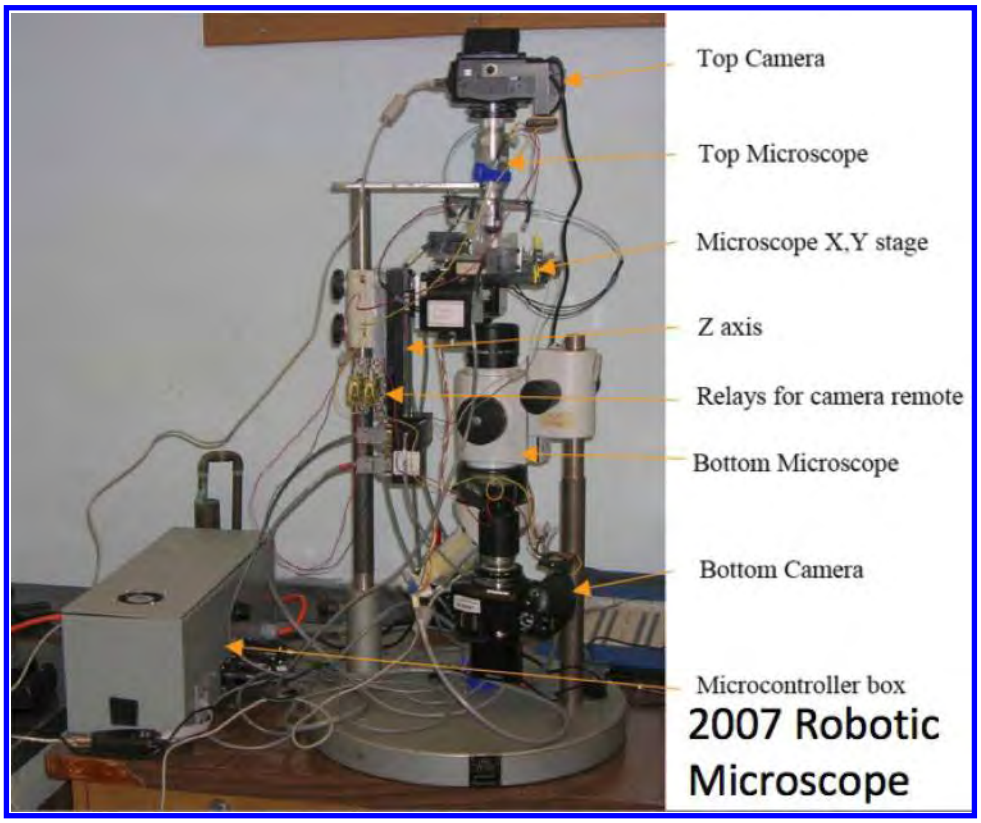

Figure 11.
The assembled robotic microscope (Crawford-Young 2007), with permission.

long working distance microscopes based on their telescope design, in the 1980s (Questar 2000) with a resolution of 1.1 μm at a 15-cm working distance. However, there is now a new set of microscope objectives, designed for industrial nondestructive testing, with the remarkable characteristics of having both the limiting resolution of light microscopy (0.5 μm) and long working distances, 13 mm for the 50 $\times$ (Edmund Optics).

The long working distance permits intervening optics between the objective and the embryo, used to obtain multiple views. We will replace the prisms by front surface mirrors to

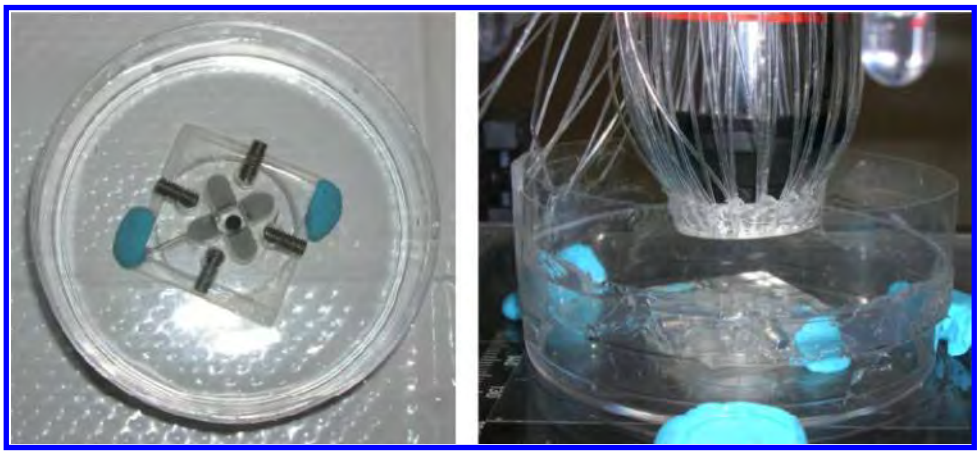

Figure 12.
Fiber optic illumination of the top water immersion objective in the robotic microscope (Crawford-Young 2007), with permission.

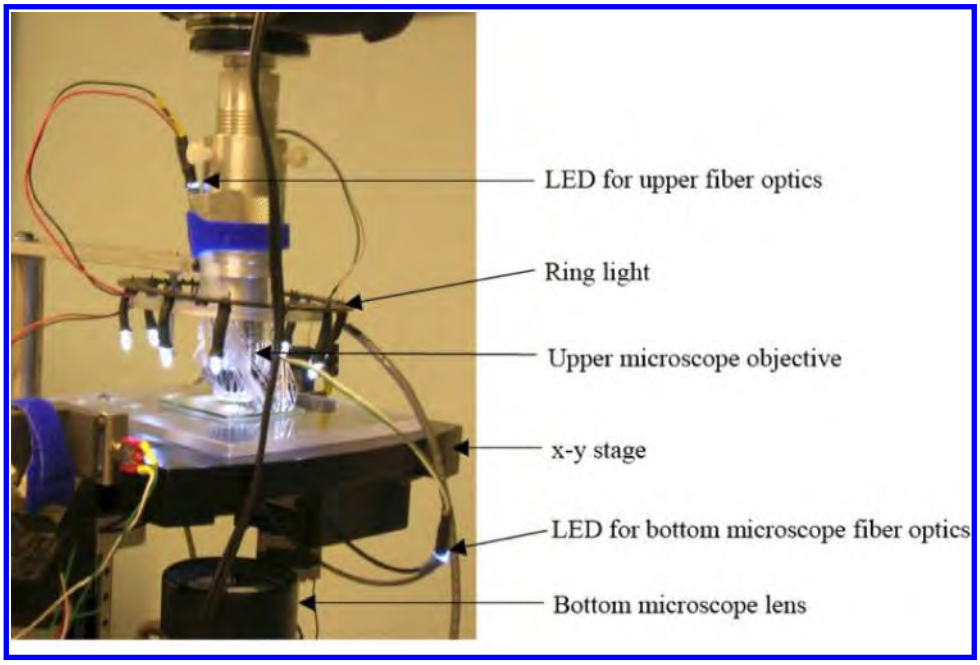

Figure 13.
Ring and bottom illuminators for the robotic microscope (Crawford-Young 2007), with permission.

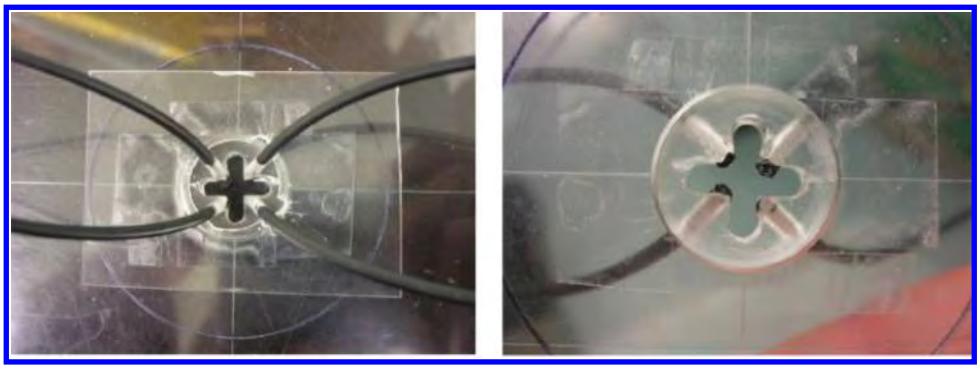

Figure 14.
Top and bottom views of the fiber optic illumination aimed between the four prisms (Crawford-Young 2007), with permission.

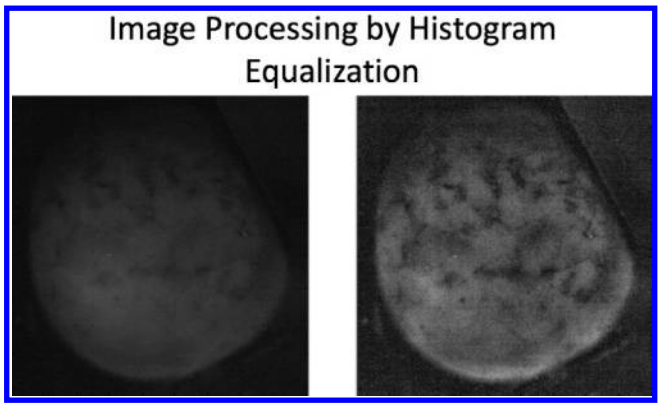

Figure 15.
An axolotl image before and after histogram equalization (Crawford-Young 2007).

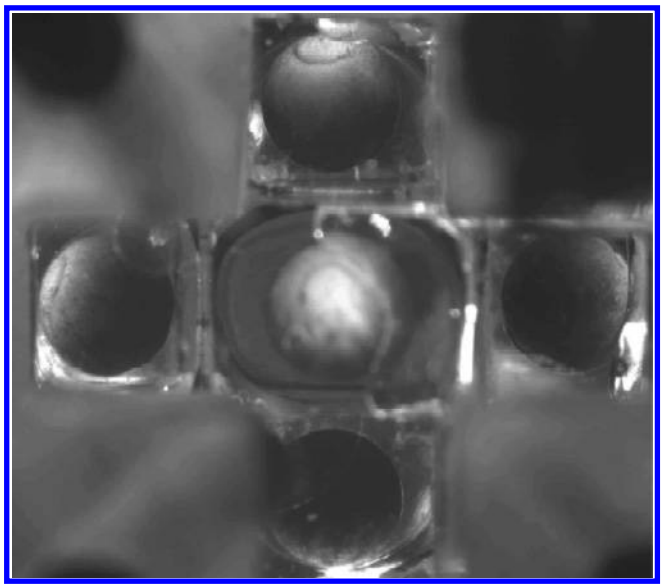

Figure 16.
Five bottom views of an axolotl. Note that the central image is out of focus while the four side views are in focus, due to the difference in optical path length (which includes physical distance divided by refractive index) (Crawford-Young 2007).

avoid spherical and other aberrations, and use epi-illumination for uniform lighting. Monochromatic blue light emitting diode illumination will be used, which matches one of the colors that the objective is corrected for, and being a short wavelength (0.470 μm) gives higher resolution than white light. Due to the narrow depth of focus of the objective (0.9 μm), rapid image acquisition may require spiral or other scanning algorithms for each view. Continual checking for focus will be necessary, along with montaging after data collection to retain only in focus surface voxels. That we can get surface voxels directly, and their (x, y, z) position, is due to the narrow depth of focus itself. This means that nonspherical embryos could be directly rendered in 3D. A high-speed camera will be needed to keep up with the scanning, and terabyte storage will be needed, followed by extensive processing to create the time-lapse succession of 3D images. Gigapan software modified for nonplanar surfaces might be a starting point (Sims and Dodson 2008; Sargent 2009; Schott 2009; Gibson 2010). With a high speed camera and robotics, we hope to get full surface coverage in under a minute, though with differentiation waves moving at 3 μm/min (Brodland et al. 1994), methods for time interpolation may have to be developed (Blackstock 2008). Further robotics to handle a few embryos at a time would obviate the problem of a defective or infected embryo, allow an understanding of individual variability, allow for control versus manipulated embryos, and create the opportunity to use more than one embryo per spawning. We have to trade off the cost of a second objective and camera for the top view versus swinging a single objective between top and bottom viewing. The mirrors could be arranged for three images up and three down, allowing parallel image capture top and bottom.

For a spherical embryo, the in-focus regions of consecutive images will be annuli whose thickness corresponds to the depth of focus, similar to annuli of a Fresnel lens. These in-focus steps can therefore be approximately predicted for a real embryo, and thus tracked with the (x, y, z) motion of the stage, reducing image acquisition time.

With the radius of an axolotl embryo at 1 mm, the number of pixels needed to cover the whole surface at 0.5 μm is 4π (1000 μm)^2/(0.5 μm)^2 = 50 megapixels, about the same as that of a single image from a present high end digital camera. If we assume that at these early stages of embryogenesis half the cells are on the outside surface, then each of the 20,000 surface cells would be recorded as an average of 25 $\times$ 25 pixels at neural tube closure, and more at earlier stages, when there are fewer, larger cells. This is quite reasonable for shape, cell division, and other details. Thus every cell could be seen clearly at this resolution and easily tracked. Because axolotl embryo cells have variegated pigmentation (Figure 18), this additional cue is available to uniquely identify each cell, and for fusing images (as is done in panoramic photography, such as Gigapan). The dataset obtained would therefore be much richer than modern attempts to merely track the nuclei of cells in embryos (Keller et al. 2008), in which no other anatomical properties of the cells can be observed.

As each surface voxel is typically viewed from three directions, we have the choice of either speeding processing by ignoring it after the first time, or better of combining the data using direction cosines. The latter could be calculated from the actual local surface angles instead of assuming embryo sphericity. As the depth of focus (0.9 μm) is nearly twice the lateral resolution (0.5 μm), there is also an opportunity here to achieve isotropic resolution in 3D despite the anisotropic resolution of the optics. The trick is to realize that each surface voxel, as seen in the three directions combined, is represented by a toy jack shaped point spread function (PSF) (consisting of three mutually perpendicular line segments). The

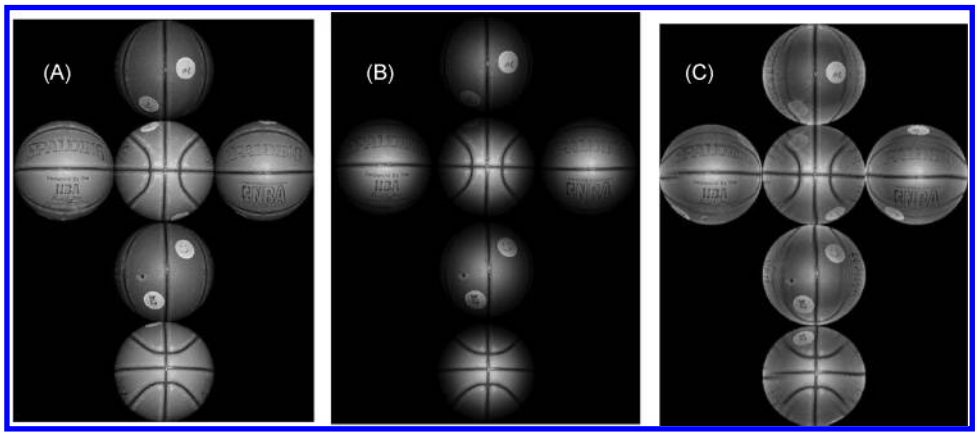

Figure 17.
(A) Views of a sphere (a basketball) from which a surface rendition is reconstructed (Tsang and Kler 2002). (B) Each projected view becomes less and less significant as it moves away from the center. The fading of pixels in one view corresponds to brighter pixels in corresponding views. This weighted grayscale scheme allows for the view with the most direct view of the pixel (voxel) to have the most significance on its grayscale value. (C) Projections of six hemispheres of the rendered basketball back onto the six faces of the box containing it. Used with permission.

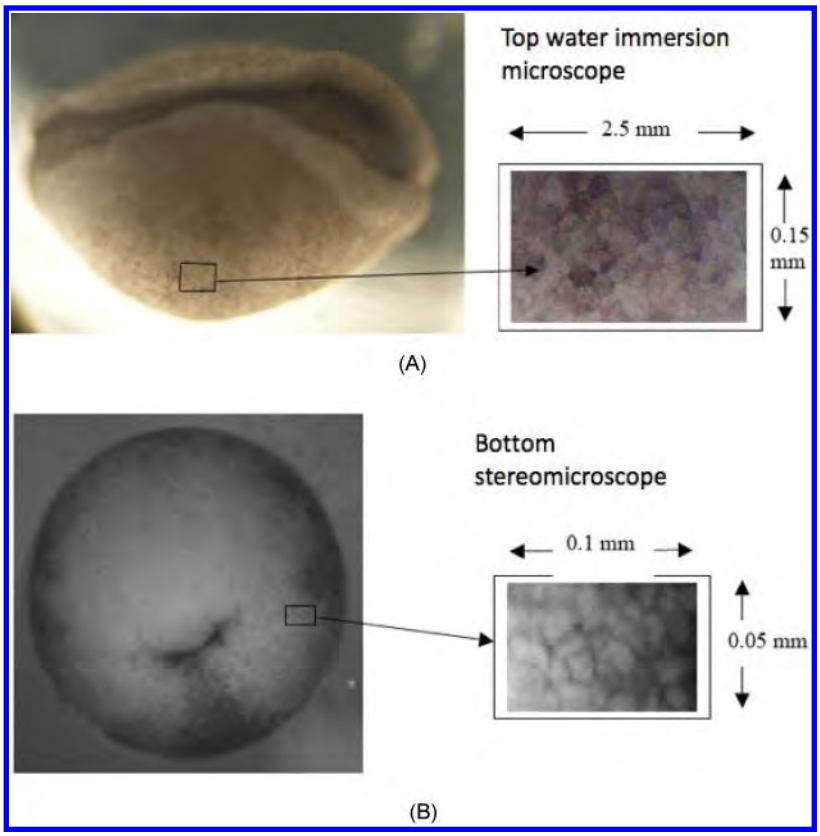

Figure 18.
Cellular resolution is achieved by the axolotl robotic microscope, with 1.2-μm pixels (Crawford-Young 2007), with permission.

deconvolution of similar, albeit 2D x-shaped PSFs, has been accomplished by Wiener filtration (Dhawan et al. 1984, 1985).

An even more precise approach can be had using the generalized algebraic reconstruction technique algorithm, which can handle simultaneous equations representing any linear combination of voxels (Gordon 1974). Consider the 3 × 3 cube of voxels around a given voxel at (a, b, c), with camera pixel measurements from three perpendicular directions of (X_{abc}, Y_{abc}, Z_{abc}). Let ρ_{ijk} be the unknown value to be assigned to voxel (i, j, k). Then for each voxel we have the following:

$$X_{a,b,c} = \frac{1-w}{2}\rho_{a-1,b,c} + w\rho_{a,b,c} + \frac{1-w}{2}\rho_{a+1,b,c}$$

$$Y_{a,b,c} = \frac{1-w}{2}\rho_{a,b-1,c} + w\rho_{a,b,c} + \frac{1-w}{2}\rho_{a,b+1,c}$$

$$Z_{a,b,c} = \frac{1-w}{2}\rho_{a,b,c-1} + w\rho_{a,b,c} + \frac{1-w}{2}\rho_{a,b,c+1}$$

where w is the weight assigned to the central voxel. A more general formulation would take into account the double cone beam PSF of the objective lens (Gordon 1983). Those voxels that are known to be more than a pixel or two from the tracked surface could *a priori* be set to $\rho_{abc} = 0$, so the calculation iteratively solving the above set of equations for the ρ_{abc} need not proceed over the whole volume, but only over the surface voxels and their nearest neighbors.

Anticipation

As with Ganymede and the other moons of Jupiter (Gordon and Westfall 2009), we can only anticipate, but not really expect to know in advance, what we would see when we finally have an up close image of the ever changing surface of an embryo. We can expect that the reality will far exceed our present preconceptions.

There are various tools available for probing the embryo surface. Axial epi-illumination could be used for fluorescence imaging of specific gene products produced during steps of differentiation, or for ultraviolet (UV) or laser microbeam surgery (Uretz et al. 1954; Berns 1974; Berns et al. 1991). The open access at least to the top of the embryo permits further experiments in micromanipulation, topical local application of drugs, such as cytoskeletal inhibitors via narrow capillaries, and the measurement of electric potentials of the cells. Thus the robotic microscope is adaptable to a number of future experiments, which could permit the integration of molecular biology and electrophysiology with mechanical and visual approaches. For example, differentiation waves have been hypothesized to be calcium waves (Jaffe 1995), and thus should have an ionic current component.

Google Embryo Anticipations

Here are some detailed questions that I am particularly interested in:

(1) Early development occurs mostly via epithelia. These sheets of cells have to remain intact while dividing into smaller and smaller cells. Consider two daughter cells resulting from a cell division. Do they stick together, or do they drift apart? If so, how far apart do they get? How is the integrity of the epithelium maintained as the cells move apart? Is the process completely passive, the cells being shorn apart, or do they appear to actively migrate among one another in any sense? Do their motions apart exhibit the mirror symmetry that has been observed for daughter cells *in vitro* (Albrecht-Buehler 1977)? Does shear ever isolate cells from a sheet, as possibly in the formation of germ cells (Björklund and Gordon 1994) or the neural crest? With the data from the new robotic microscope we should be able to track the distance apart versus time of many pairs of daughter cells, and build up a quantitative idea of how much cell dispersion or mixing occurs. Does

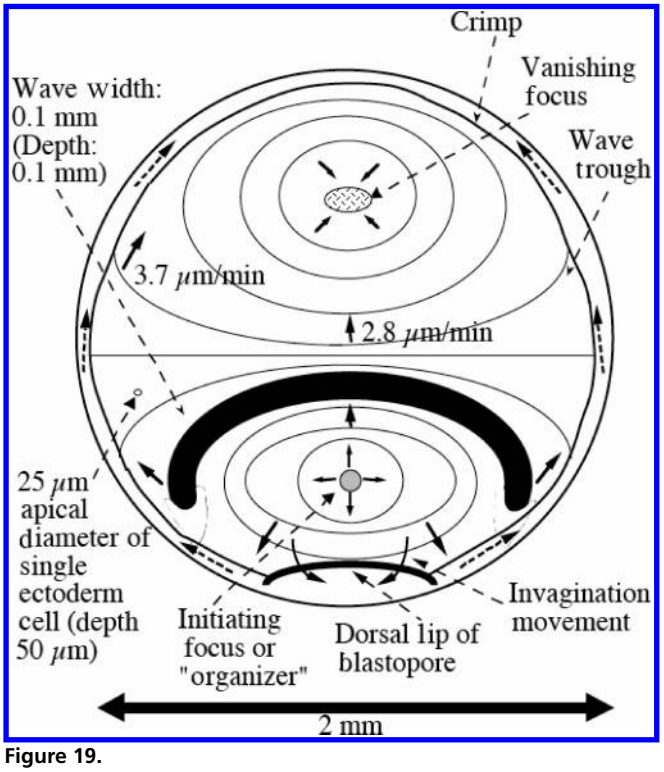

Figure 19.
In 1985, I predicted that differentiation of ectoderm to neuroepithelium was triggered by a wave of contraction carried by a cytoskeletal apparatus that I called the cell state splitter (Gordon and Brodland 1987), and the predicted wave was found in 1990 by Natalie K. Björklund (Gordon 1999) and confirmed in our collaborators' lab (Brodland et al. 1994). No more than a stereomicroscope and 10,000x time-lapse imaging were needed to see these waves (Gordon and Björklund 1996). The wave that leaves the neuroepithelium in its wake is 0.1-mm wide and deep, traversing one hemisphere of the ectoderm in 12 hr via a strange trajectory that starts at a point, then travels as an ellipse until it hits the dorsal lip of the blastula. That portion vanishes but the remaining arc changes from convex to concave and converges upon itself at the future head end of the embryo, where it vanishes as if it were a wave in an active medium, which may be precisely what it is. Reproduced with permission of Elsevier.

the separation of cells versus time exhibit the properties of chaotic advection or mixing (Karniadakis et al. 2005)? What is the variability between individuals in which cells go where? Do the cells form compartment boundaries, such as have been observed in insect development (Dahmann and Basler 1999)? (2) Visible waves of differentiation propagate through embryos (Foe and Alberts 1983; Foe 1989; Foe and Odell 1989; Brodland et al. 1994; Gordon et al. 1994; Gordon and Björklund 1996; Gilland et al. 1999, 2003; Webb and Miller 2003), linking cell level behavior to the genome (Gordon 1999). Differentiation waves may be the key to understanding cell differentiation in general and may be the basis for macroevolution (Gordon 1999). Our working hypothesis is that a mechanical wave of contraction or expansion of the apical surfaces of cells in embryonic epithelia triggers signal transduction that alters the differentiated state of the cells through which the wave propagates (Gordon 1999). The trajectory of the wave that leaves in its wake the neural plate is

given in Figure 19. Note that its speed is greater at the edge than in the middle, so that it changes from convex to concave as it travels. We have suggested that alterations in the speed of the wave, perhaps due to DNA methylation deficiency, may be the cause of neural tube defects (Björklund and Gordon 2006). I, therefore, want to determine whether, when a neural tube defect (NTD) is taking place (Lee et al. 1988), it is preceded by an aberrant differentiation wave. NTDs are among the most common serious human birth defects.

(3) The local speed of the wave may depend on some local property of the epithelium through which it is propagating. I hypothesize that the key property is the strain state of the local tissue. This can be characterized in at least two ways: by the stretching of the cells in a given direction (Jacobson and Gordon 1976a) and by the rate of change of the great circle distance between pairs of cells. We could thus make maps of orientation (Ayres and Rangayyan 2007) and strain over the whole surface of the embryo, and see if they correlate with the speed of differentiation waves over the surface.

(4) In the fruit fly *Drosophila*, differentiation is accompanied 100% with waves of cell division called mitotic waves (Foe and Alberts 1983; Foe 1989; Foe and Odell 1989). I would like to determine if there is any correlation between differentiation waves and cell division over the surface of the axolotl embryo.

(5) One unsolved problem about differentiation waves is that we do not yet know if specific physical and/or chemical events trigger them. A close-up analysis of the launching sites of differentiation waves may provide clues to the mechanism.

(6) I have hypothesized that at any stage of embryogenesis, stem cells are those cells that are at a border between the trajectories of pairs of differentiation waves and are thus stuck at a given stage of differentiation because they have participated in neither an expansion nor a contraction wave (Gordon 2006). Whether such cells exist, which are missed by a pair of waves, could be determined from Google Embryo datasets, and by tracking them to later stages of embryogenesis, we could find out if they somehow avoid participation in all subsequent differentiation waves. Isolation of them could determine their degree of pleuripotency.

Conclusion and Future Prospects

I am not alone in this view of the path ahead:

> We argue here that imaging can play a vital role in systems biology, offering a path from rough static models to more refined, quantitative dynamic models. In vivo imaging can capture quantitative data at single-cell resolution and do so noninvasively as the biological circuit functions, offering insights that cannot be matched using in vitro approaches. With the emergence of automated instrumentation and advanced analysis tools, such intravital imaging has become practical for both hypothesis driven research and high-throughput discovery science. (Megason and Fraser 2007: 784)

> The analysis of massive image databases can be greatly facilitated by computer vision techniques once annotated image sets reach the crucial mass sufficient to train the computer in pattern recognition. Ultimately, genome-wide atlases of gene expression during development will record gene activity in living animals with at least cellular resolution and in the context of morphogenetic events. These emerging datasets will lead to great advances in the field of comparative genomics and revolutionize our ability to decipher and model developmental processes for a variety of organisms. (Lécuyer and Tomancak 2008: 506)

> Quantitative mapping of the normal tissue dynamics of an entire developing mammalian organ has not been achieved so far but is essential to understand developmental processes and to provide quantitative data for computational modeling. (Boot et al. 2008: 609).

> A long-standing goal of biology is to map the behavior of all cells during vertebrate embryogenesis. . . . Our digital embryos, with 55 million nucleus entries, are provided as a resource. (Keller et al. 2008: 1065)

As with the planets and their moons, we would like knowledge that is more than skin deep. Some embryologists turn to transparent embryos (Sampetrean et al. 2009; Keller et al. 2008) in the hope of accomplishing such in-depth imaging, but the very transparency makes the cells and their changing shapes nearly invisible without interferometric or fluorescence techniques, which obfuscate the transparent cells due to their overlapping. We are experimenting with microMRI (magnetic resonance imaging) (Gruwel et al. 2008) and considering x-ray microCT (computed tomography) (Boughner et al. 2007), which are applicable to visually opaque embryos, but have not yet reached the resolution of light microscopy. There are prospects for multiphoton confocal microscopy, optical coherence tomography, and Shack-Harman optics (Molebny et al. 1998). An example of a question requiring in-depth, cellular level imaging is: where is the wave in the South African clawed toad *Xenopus laevis* (Nieuwkoop et al. 1996) that corresponds to that in axolotl, shown in Figure 19? Because the ectoderm is covered by an extra layer of cells in frogs and toads (the superficial epithelium), this wave may be obscured. So other methods besides simple time-lapse microscopy of the embryo's surface will be needed to see if the predicted wave is there. Perhaps, as in the eye development of the flour beetle, *Tribolium*, in which the eye imaginal discs are similarly covered (Friedrich et al. 1996), the wave is at the bottom (basal) end of the cells, rather than at the apical end.

Biologists have a tendency not to look at that which they cannot see. In the case of embryos, a blatant example is the rather extensive electric currents that loop in and out of embryos. I reviewed the fields that have been noted in fertilized eggs since 1905 (Gordon 1999 section 9.27).

The following observations are from Table 2 of Jaffe and Nuccitelli (1977) in regard to the "inferred steady current direction," which

(1) leaves animal pole, enters vegetal pole during maturation of the turtle egg, *Chrysamys* (Hyde 1905);
(2) enters animal pole, leaves vegetal pole during 45 min before first cleavage of the fish egg, *Fundulus* (Hyde 1905);
(3) enters animal pole, leaves equator between fertilization and first cleavage of the frog egg, *Rana* (Burr 1941; cf. Burr 1932; Burr and Northrop 1935, 1939; Burr and Hovland 1937; Burr and Bullock 1941; Burr and Sinnott 1944);
(4) enters animal pole and sperm entry point, leaves vegetal pole between fertilization and 1st cleavage of the urodele egg, *Hynobius nebulosus* (Hasama 1935);
(5) enters animal pole, leaves vegetal pole after fertilization during cytoplasmic segregation of the fish egg, *Oryzias latipes* (Jaffe and Nuccitelli 1977: 452).

Although some of these observations doubtless bear repeating, and should be taken to later stages of development, such as midblastula transition, we see that it is plausible that the animal pole has a current going through it.

The development of electrical impedance tomographic microscopy (Griffiths et al. 1996) may someday help tackle these aspects of embryogenesis.

An actual landing on Ganymede, as the landings on the Moon and Mars have proven, would go well beyond "mere" imaging from a distance, however close. So I will end by proposing an actual landing on living embryos that leaves at most "footprints." This might be accomplished on the surface by near-field optics (Courjon 2003) and inside the embryo by cytobots (Chrusch et al. 2001).

While, as shown by Bowman (2009), we generally do not see what we are not looking for, deliberate exploration into the unknown opens our eyes to new possibilities.

Acknowledgments

I would like to thank Fred Bookstein for extending an invitation to attend the 19th Altenberg Workshop in Theoretical Biology on "Measuring Biology" in 2008, William R. Buckley and John E. Westfall for critical readings, and Susan Crawford-Young (Red River College), Stephen P. McGrew (New Light Industries, Spokane), and Ian Paul and Rick Howard (Medical Devices, CancerCare Manitoba) for past and recent discussions. This work was supported in part by CancerCare Manitoba, Manitoba Institute of Child Health, the Canadian Space Agency, and the New Light Industries.

Note

1. The history of embryology is rife with claims varying from a homunculus-like map of the future organism to total lack of a map at these early stages, and everything in between. My assessment is that just fertilized one-cell embryos are fundamentally spherically symmetric. Testing this concept one way or the other is a challenge.

I keep a breeding colony of axolotls (see Figure 2) for their embryos, because they are easy to handle, being neotenic salamanders that become sexually mature in the larval form. They breathe underwater using external gills, mate there, and can be maintained much like aquarium fish. Females produce about 300 eggs four times a year. Their spherical eggs are huge for eggs that do not contain a separate yolk, at 2-mm diameter (23,000 × the volume of human eggs). Yolk platelets are inside each cell, with 70% initially in the lower, "vegetal" hemisphere at the one-cell stage (Kalthoff 2001), suggesting some transport of nutrition between cells as cleavage proceeds. While the cells get smaller because there is no external source of nutrition, at the stage of neural tube closure, when the "major events" (depending on one's viewpoint) of embryogenesis have all occurred, the cells are still 15-μm wide and 50-μm tall, about 100 times the volume of a typical mammalian cell. At this stage, the axolotl contains a mere 40,000 cells (Gillette 1944), about half visible on the outer surface. In amphibians, even fewer, larger cells at any stage could be had by inducing polyploidy (Fankhauser 1941, 1945; Fankhauser and Schott 1952; Fankhauser et al. 1955; Gordon 1999), whereas mammalian embryos appear to divide down to a minimum cell size (Feng and Gordon 1997) and perhaps keep that cell size subsequently. Human polyploids are not viable (Rowlands and Hwang 1998). A transition in rate of cell division occurs in amphibian embryogenesis (Wang et al. 2000).

The axolotl has its own community of scientists and genome project (Putta et al. 2004; Smith et al. 2005). We have the only breeding colony in Canada, which has been functioning since 1990, and have contributed to a handbook (Gordon and Brodland 1989) and pioneered humane husbandry of these animals (Björklund 1993).

References

Aguet F, Van De Ville D, Unser M (2008) Model-based 2.5-d deconvolution for extended depth of field in brightfield microscopy. IEEE Transactions on Image Processing 17: 1144–1153.

Albrecht-Buehler G (1977) Daughter 3T3 cells: Are they mirror images of each other? Journal of Cell Biology 72: 595–603.

Asada-Kubota M, Kubota HY (1991) Furrow-related contractions are inhibited but furrow-unrelated contractions are not affected in *af* mutant eggs of *Xenopus laevis*. Developmental Biology 147: 354–362.

Austin RH, Chan SS (2003) Of spherical cows, cloudy crystal balls, and proteins. Biochemical and Biophysical Research Communications 312: 215–221.

Ayres FJ, Rangayyan RM (2007) Design and performance analysis of oriented feature detectors. Journal of Electronic Imaging 16(2): article number 023007, 12 pages.

Banchoff TF (1990) Beyond the Third Dimension: Geometry, Computer Graphics, and Higher Dimensions. New York: Scientific American Library.

Beloussov LV, Gordon R (2006) Preface. Morphodynamics: Bridging the gap between the genome and embryo physics. International Journal of Developmental Biology 50: 79–80.

Berns MW (1974) Biological Microirradiation: Classical and Laser Sources. Englewood Cliffs, NJ: Prentice-Hall.

Berns MW, Wright WH, Wiegand Steubing R (1991) Laser microbeam as a tool in cell biology. International Review of Cytology 129: 1–44.

Björklund NK (1993) Small is beautiful: Economical axolotl colony maintenance with natural spawnings as if axolotls mattered. In: Handbook on Practical Methods (Malacinski GM, Duhon ST, eds), Bloomington, IN: Department of Biology, Indiana University, 38–47.

Björklund NK, Gordon R (1994) Surface contraction and expansion waves correlated with differentiation in axolotl embryos. I. Prolegomenon and differentiation during the plunge through the blastopore, as shown by the fate map. Computers and Chemistry 18: 333–345.

Björklund NK, Gordon R (2006) A hypothesis linking low folate intake to neural tube defects due to failure of post-translation methylations of the cytoskeleton. International Journal of Developmental Biology 50: 135–141.

Blackstock A (2008) Intelligent Image Segmentation Using Uniform-Cost Search. Moffett Field, CA: NASA Ames Research Center. Available at http://www.alexblackstock.com/professional/writing.html

Boot MJ, Westerberg CH, Sanz-Ezquerro J, Cotterell J, Schweitzer R, Torres M, Sharpe J (2008) *In vitro* whole-organ imaging: 4D quantification of growing mouse limb buds. Nature Methods 5: 609–612.

Bordzilovskaya NP, Dettlaff TA (1979) Table of stages of the normal development of axolotl embryos and the prognostication of timing of successive developmental stages at various temperatures. Axolotl Colony Newsletter 7: 2–22.

Bordzilovskaya NP, Dettlaff TA, Duhon ST, Malacinski GM (1989) Developmental-stage series of axolotl embryos. In: Developmental Biology of the Axolotl (Armstrong JB, Malacinski GM, eds), 201–219. New York: Oxford University Press.

Boterenbrood EC, Narraway JM (1986) The direction of cleavage waves and the regional variation in the duration of cleavage cycles on the dorsal side of the *Xenopus laevis* blastula. Roux's Archives of Developmental Biology 195: 484–488.

Boterenbrood EC, Narraway JM (1990) Epiboly connected with cleavage in morula and early blastula stages of *Xenopus laevis*, a study using time-lapse photography. Roux's Archives of Developmental Biology 198: 303–307.

Boterenbrood EC, Narraway JM, Hara K (1983) Duration of cleavage cycles and asymmetry in the direction of cleavage waves prior to gastrulation in *Xenopus laevis*. Roux's Archives of Developmental Biology 192: 216–221.

Boughner JC, Buchtova M, Fu K, Diewert V, Hallgrimsson B, Richman JM (2007) Embryonic development of *Python sebae*. I: Staging criteria and macroscopic skeletal morphogenesis of the head and limbs. Zoology (Jena) 110: 212–230.

Bowman CE (2009) Megavariate genetics: What you find is what you go looking for. Biological Theory 4: 21–28.

Brodland GW, Gordon R, Scott MJ, Björklund NK, Luchka KB, Martin CC, Matuga C, Globus M, Vethamany-Globus S, Shu D (1994) Furrowing surface contraction wave coincident with primary neural induction in amphibian embryos. Journal of Morphology 219: 131–142.

Brodland GW, Scott MJ, MacLean AF, Globus M, Vethamany-Globus S, Gordon R, Veldhuis JH, Del Maestro R (1996) Morphogenetic movements during axolotl neural tube formation tracked by digital imaging. Roux's Archives of Developmental Biology 205: 311–318.

Brodland GW, Veldhuis JH (1998) Three-dimensional reconstruction of live embryos using robotic macroscope images. IEEE Transactions on Biomedical Engineering 45: 1173–1181.

Burnside MB, Jacobson AG (1968) Analysis of morphogenetic movements in the neural plate of the newt *Taricha torosa*. Developmental Biology 18: 537–552.

Burr HS (1932) An electro-dynamic theory of development suggested by studies of proliferation rates in the brain of *Amblystoma*. Journal of Compatative Neurology 56: 347–371.

Burr HS (1941) Field properties of the developing frog's egg. Proceedings of the National Academy of Sciences USA 27: 276–281.

Burr HS, Bullock TH (1941) Steady state potential differences in the early development of *Amblystoma*. Yale Journal of Biology and Medicine 14: 51–57.

Burr HS, Hovland CI (1937) Bioelectric correlates of development in *Amblystoma*. Yale Journal of Biology and Medicine 9: 541–549.

Burr HS, Northrop FSC (1935) The electro-dynamic theory of life. Quarterly Review of Biology 10: 322–333.

Burr HS, Northrop FSC (1939) Evidence for the existence of an electro-dynamic field in living organisms. Proceedings of the National Academy of Sciences USA 25: 284–288.

Burr HS, Sinnott EW (1944) Electrical correlates of form in cucurbitfruits. American Journal of Botany 31: 249–253.

Caron N, Sheng Y (2008) Polynomial phase masks for extending the depth of field of a microscope. Applied Optics 47(22): E39–43.

Chan M (1997) Egon Schiele: The Leopold Collection Vienna. MoMA (Museum of Modern Art)(26), 2–7. Available at http://www.moma.org/interactives/exhibitions/1997/schiele/artistwork.html

Chen X, Brodland GW (2008) Multi-scale finite element modeling allows the mechanics of amphibian neurulation to be elucidated. Physical Biology 5, doi:10.1088/1478–3975/1085/1081/015003

Chrusch DD, Podaima BW, Gordon R (2001) Cytobots: Intracellular robotic micromanipulators. Canadian Conference on Electrical and Computer Engineering, 2002. IEEE CCECE 2002, Piscataway: IEEE, 1640–1645.

Courjon D (2003) Near-Field Microscopy and Near-Field Optics. Singapore: World Scientific.

Crawford-Young S (2007) A Robotic Microscope for 3D Time-Lapse Imaging of Early Stage Axolotl Salamander Embryos. M.Sc. Thesis, Department of Electrical and Computer Engineering, University of Manitoba, Winnipeg. Available at http://mspace.lib.umanitoba.ca/bitstream/1993/331/1/MSc%20Thesis%20Susan%20Crawford–Young%202007.pdf

Dahmann C, Basler K (1999) Compartment boundaries at the edge of development. Trends in Genetics 15: 320–326.

Dhawan AP, Rangayyan RM, Gordon R (1984) Wiener filtering for deconvolution of geometric artifacts in limited-view image reconstruction. Proceedings of SPIE 515: 168–172.

Dhawan AP, Rangayyan RM, Gordon R (1985) Image restoration by Wiener deconvolution in limited-view computed tomography. Applied Optics 24: 4013–4020.

Dowski E Jr, Johnson G (2002) Marrying optics and electronics. Aspheric optical components and electronics improve depth of field for imaging systems. SPIE's OE Magazine (Jan), 42–43.

Doyle J (2001) Computational biology: Beyond the spherical cow. Nature 411: 151–152.

Eliceiri KW, Thomas C, White JG (2000) 4D Software Suite: Software tools for the capture and analysis of 4-dimensional data sets. Early 2000 Midwest Worm Meeting, abstract 57.

Elul T, Koehl MA, Keller R (1997) Cellular mechanism underlying neural convergent extension in *Xenopus laevis* embryos. Developmental Biology 191: 243–258.

Evsikov SV, Morozova LM, Solomko AP (1994) Role of ooplasmic segregation in mammalian development. Roux's Archives of Developmental Biology 203: 199–204.

Ewald AJ, Peyrot SM, Tyszka JM, Fraser SE, Wallingford JB (2004) Regional requirements for Dishevelled signaling during *Xenopus* gastrulation: Separable effects on blastopore closure, mesendoderm internalization and archenteron formation. Development 131: 6195–6209.

Fankhauser G (1941) Cell size, organ and body size in triploid newts (*Triturus viridescens*). Journal of Morphology 68: 161–177.

Fankhauser G (1945) The effect of changes in chromosome number on amphibian development. Quarterly Review of Biology 20: 20–78.

Fankhauser G, Schott BW (1952) Inverse relation of number of melanophores to chromosome number in embryos of the newt, *Triturus viridescens*. Journal of Experimental Zoology 121: 105–119.

Fankhauser G, Vernon JA, Frank WH, Slack WV (1955) Effect of size and number of brain cells on learning in larvae of the salamander, *Triturus viridescens*. Science 122: 692–693.

Feng YL, Gordon JW (1997) Removal of cytoplasm from one-celled mouse embryos induces early blastocyst formation. Journal of Experimental Zoology 277: 345–352.

Fire A (1994) A four-dimensional digital image archiving system for cell lineage tracing and retrospective embryology. Computer Applications in the Biosciences 10: 443–447.

Fleming TP, Papenbrock T, Fesenko I, Hausen P, Sheth B (2000) Assembly of tight junctions during early vertebrate development. Seminars in Cell and Developmental Biology 11: 291–299.

Foe VE (1989) Mitotic domains reveal early commitment of cells in *Drosophila* embryos. Development 107: 1–22.

Foe VE, Alberts BM (1983) Studies of nuclear and cytoplasmic behaviour during the five mitotic cycles that precede gastrulation in *Drosophila* embryogenesis. Journal of Cell Science 61: 31–70.

Foe VE, Odell GM (1989) Mitotic domains partition fly embryos, reflecting early cell biological consequences of determination in progress. American Zoologist 29: 617–652.

Forgacs G, Newman SA (2005) Biological Physics of the Developing Embryo. Cambridge: Cambridge University Press.

Forster B, Van De Ville D, Berent J, Sage M, Unser M (2004) Complex wavelets for extended depth-of-field: A new method for the fusion of multichannel microscopy images. Microscopy Research and Technique 65: 33–42.

Friedrich M, Rambold I, Melzer RR (1996) The early stages of ommatidial development in the flour beetle *Tribolium castaneum* (Coleoptera; Tenebrionidae). Development Genes and Evolution 206: 136–146.

Gamow G (1970) My World Line: An Informal Autobiography. New York: Viking Adult.

Gibson M (2010) Nano GigaPan: Changing the Way You See. Available at http://nanogigapan.blogspot.com/

Gilland E, Baker R, Denk W (2003) Long duration three-dimensional imaging of calcium waves in zebrafish using multiphoton fluorescence microscopy. Biological Bulletin 205: 176–177.

Gilland E, Miller AL, Karplus E, Baker R, Webb SE (1999) Imaging of multicellular large-scale rhythmic calcium waves during zebrafish gastrulation. Proceedings of the National Academy of Sciences of the USA 96: 157–161.

Gillette R (1944) Cell number and cell size in the ectoderm during neurulation (*Ambystoma maculatum*). Journal of Experimental Zoology 96: 201–222.

Gordon R (1974) A tutorial on ART (Algebraic Reconstruction Techniques). IEEE Transactions on Nuclear Science NS 21: 78–93, 95.

Gordon R (1982) Rotating microscope for "LANDSAT" photography of vertebrate embryos. Proceedings of SPIE 361: 48–52.

Gordon R (1983) Computational embryology of the vertebrate nervous system. In: Computing in Biological Science (Geisow M, Barrett A, eds), 23–70. Amsterdam: Elsevier/North-Holland.

Gordon R (1999) The Hierarchical Genome and Differentiation Waves: Novel Unification of Development, Genetics and Evolution. Singapore: World Scientific; London: Imperial College Press.

Gordon R (2006) Mechanics in embryogenesis and embryonics: Prime mover or epiphenomenon? International Journal for Developmental Biology 50: 245–253.

Gordon R, Björklund NK (1996) How to observe surface contraction waves on axolotl embryos. International Journal of Developmental Biology 40: 913–914.

Gordon R, Bjorklund NK, Nieuwkoop PD (1994) Dialogue on embryonic induction and differentiation waves. International Review of Cytology 150: 373–420.

Gordon R, Brodland GW (1987) The cytoskeletal mechanics of brain morphogenesis. Cell state splitters cause primary neural induction. Cell Biophysics 11: 177–238.

Gordon R, Brodland GW (1989) Neurulation. In: Developmental Biology of the Axolotl (Armstrong JB, Malacinski GM, eds), 62–71. New York: Oxford University Press.

Gordon R, Jacobson AG (1978) The shaping of tissues in embryos. Scientific American 238(6): 106–113.

Gordon R, Buckley WR (2010) Embryo Physics Course: An Effort in Reverse Engineering. http://embryophysics.org/

Gordon R, Westfall JE (2009) Google Embryo for building quantitative understanding of an embryo as it builds itself: I. Lessons from Ganymede and Google Earth. Biological Theory 4: 390–395.

Griffiths H, Tucker MG, Sage J, Herrenden-Harker WG (1996) An electrical impedance tomography microscope. Physiological Measurement 17 (Suppl 4A): A15–24.

Gruwel MLH, Lerner BE, Björklund NK, Gordon R (2008) Time-lapse microMRI (μMRI) of axolotl embryogenesis. In: ESMRMB Congress 2008, Valencia, Spain: October 2–4, 2008. Available at http://www.esmrmb.org/

Hammond AT, Glick BS (2000) Raising the speed limits for 4D fluorescence microscopy. Traffic 1: 935–940.

Hara K (1970) "Double camera" time-lapse micro-cinematography: Simultaneous filming of both poles of the amphibian egg. Mikroskopie 26: 181–184.

Hara K (1971) Cinematographic observation of "surface contraction waves" (SCW) during the early cleavage of axolotl eggs. Wilhelm Roux' Archiv für Entwicklungsmechanik 167: 183–186.

Hardin JD, Keller RE (1988) The Behaviour and function of bottle cells during gastrulation of *Xenopus laevis*. Development 103: 211–230.

Harte J (1988) Consider a Spherical Cow, A Course in Environmental Problem Solving. Mill Valley, CA: University Science Books.

Hasama BI (1935) Über die bioelektrischen Erscheinungen beim Furchungsprozess des Eies des *Hynobius nebulosus*/On bioelectric phenomena with the cleavage process of the egg of *Hynobius nebulosus*. Protoplasma 22: 597–606.

Heid PJ, Voss E, Soll DR (2002) 3D-DIASemb: A computer-assisted system for reconstructing and motion analyzing in 4D every cell and nucleus in a developing embryo. Developmental Biology 245: 329–347.

Hyde IH (1905) Difference in electrical potential in developing eggs. American Journal of Physiology 12: 241–275.

Jacobson AG (1980) Computer modeling of morphogenesis. American Zoologist 20: 669–677.

Jacobson AG, Gordon R (1976a) Changes in the shape of the developing vertebrate nervous system analyzed experimentally, mathematically and by computer simulation. Journal of Experimental Zoology 197: 191–246.

Jacobson AG, Gordon R (1976b) Nature and origin of patterns of changes in cell shape in embryos. Journal of Supramolecular Structure 5: 371–380.

Jacobson AG, Gordon R (1977) Nature and origin of patterns of changes in cell shape in embryos. Progress in Clinical Biological Research 17: 323–332.

Jaffe LF (1995) Calcium waves and development. CIBA Foundation Symposium 188, 4–17.

Jaffe LF, Nuccitelli R (1977) Electrical controls of development. Annual Review of Biophysics and Bioengineering 6: 445–476.

Johnson MH (2009) From mouse egg to mouse embryo: Polarities, axes, and tissues. Annual Review of Cell and Developmental Biology 25: 483–512.

Kalthoff KO (2001) Analysis of Biological Development. Columbus, OH: McGraw-Hill.

Karniadakis G, Beskok A, Aluru N (2005) Microflows and Nanoflows: Fundamentals and Simulation. New York: Springer.

Keller RE (1978) Time-lapse cinemicrographic analysis of superficial cell behavior during and prior to gastrulation in *Xenopus laevis*. Journal of Morphology 157: 223–248.

Keller RE (1981) An experimental analysis of the role of bottle cells and the deep marginal zone in gastrulation of *Xenopus laevis*. Journal of Experimental Zoology 216: 81–101.

Keller RE, Cooper MS, Danilchik M, Tibbetts P, Wilson PA (1989) Cell intercalation during notochord development in *Xenopus laevis*. Journal of Experimental Zoology 251: 134–154.

Keller RE, Danilchik M (1988) Regional expression, pattern and timing of convergence and extension during gastrulation of *Xenopus laevis*. Development 103: 193–209.

Keller RE, Danilchik M, Gimlich R, Shih J (1985) The function and mechanism of convergent extension during gastrulation of *Xenopus laevis*. Journal of Embryology and Experimental Morphology 89 (Suppl.): 185–209.

Keller RE, Hardin J (1987) Cell behaviour during active cell rearrangement: Evidence and speculations. Journal of Cell Science 8 (Suppl.): 369–393.

Keller PJ, Schmidt AD, Wittbrodt J, Stelzer EHK (2008) Reconstruction of zebrafish early embryonic development by scanned light sheet microscopy. Science 322: 1065–1069.

Keller R, Shih J, Sater A (1992) The cellular basis of the convergence and extension of the *Xenopus* neural plate. Developmental Dynamics 193: 199–217.

Keller RE, Spieth J (1984) Neural crest cell behavior in white and dark larvae of *Ambystoma mexicanum*: Time-lapse cinemicrographic analysis of pigment cell movement *in vivo* and in culture. Journal of Experimental Zoology 229: 109–126.

Konijn GA, Vardaxis NJ, Boon ME, Kok LP, Rietveld DC, Schut JJ (1996) 4D confocal microscopy for visualisation of bone remodelling. Pathology: Research and Practice 192: 566–572.

Lécuyer E, Tomancak P (2008) Mapping the gene expression universe. Current Opinion in Genetics and Development 18: 506–512.

Lee H, Bush KT, Nagele RG (1988) Time-lapse photographic study of neural tube closure defects caused by xylocaine in the chick. Teratology 37: 263–269.

LeSage AJ, Kron SJ (2002) Design and implementation of algorithms for focus automation in digital imaging time-lapse microscopy. Cytometry 49: 159–169.

Megason SG, Fraser SE (2007) Imaging in systems biology. Cell 130: 784–795.

Mietchen D, Jakobi JW, Richter HP (2005a) Cleavage plane reorientation in *Xenopus* early embryos: The role of cell shape. European Journal of Cell Biology 84 (Suppl. 55): 82.

Mietchen D, Jakobi JW, Richter HP (2005b) Cortex reorganization of *Xenopus laevis* eggs in strong static magnetic fields. BioMagnetic Research and Technology 3(2), doi: 10.1186/1477–1044X-1183–1182

Molebny VV, Gordon R, Kurashov VN, Podanchuk DV, Kovalenko AV, Wu J (1998) Refraction mapping of translucent objects with Shack-Harman sensor. Proceedings of SPIE 3548: 31–33.

Niehrs C, Keller R, Cho KW, De Robertis EM (1993) The Homeobox gene *goosecoid* controls cell migration in *Xenopus* embryos. Cell 72: 491–503.

Nieuwkoop PD, Björklund NK, Gordon R (1996) Surface contraction and expansion waves correlated with differentiation in axolotl embryos. II. In contrast to urodeles, the anuran *Xenopus laevis* does not show furrowing surface contraction waves. International Journal of Developmental Biology 40: 661–664.

Nikas G, Paraschos T, Psychoyos A, Handyside AH (1994) The zona reaction in human oocytes as seen with scanning electron microscopy. Human Reproduction 9: 2135–2138.

Nouri C, Luppes R, Veldman AEP, Tuszynski JA, Gordon R (2008) Rayleigh instability of the inverted one-cell amphibian embryo. Physical Biology 5(1): 015006.

Ortyn WE, Perry DJ, Venkatachalam V, Liang LC, Hall BE, Frost K, Basiji DA (2007) Extended depth of field imaging for high speed cell analysis. Cytometry 71A: 215–231.

Parichy DM (1996) When neural crest and placodes collide: Interactions between melanophores and the lateral lines that generate stripes in the salamander *Ambystoma tigrinum tigrinum* (Ambystomatidae). Developmental Biology 175: 283–300.

Pérez-Mongiovi D, Chang P, Houliston E (1998) A propagated wave of MPF activation accompanies surface contraction waves at first mitosis in *Xenopus*. Journal of Cell Science 111(Pt 3): 385–393.

Putta S, Smith JJ, Walker J, Rondet M, Weisrock D, Monaghan J, Samuels AK, Kump K, King DC, Maness NJ, Habermann B, Tanaka E, Bryant SV, Gardiner DM, Parichy FM, Voss SR (2004) From biomedicine to natural history research: Expressed sequence tag resources for ambystomatid salamanders. BMC Genomics 5(1): 54.

Questar (2000) Questar QM 100 Photo-Visual Long Distance Microscope. New Hope, PA: Questar Corporation. Available at http://www.company7.com/questar/microscope/qm100.html

Radlanski RJ, van der Linden FP, Ohnesorge I (1999) 4D-computerized visualisation of human craniofacial skeletal growth and of the development of the dentition. Annals of Anatomy 181: 3–8.

Rivera-Perez JA (2007) Axial specification in mice: Ten years of advances and controversies. Journal of Cellular Physiology 213: 654–660.

Rowlands CG, Hwang WS (1998) Cytomegaly of pancreatic D cells in triploidy. Pediatric Pathology and Laboratory Medicine 18: 49–55.

Russ JC (2002) The Image Processing Handbook. Boca Raton, FL: CRC Press.

Salihagic-Kadic A, Kurjak A, Medic M, Andonotopo W, Azumendi G (2005) New data about embryonic and fetal neurodevelopment and behavior obtained by 3D and 4D sonography. Journal of Perinatal Medicine 33: 478–490.

Sampetrean O, Iida SI, Makino S, Matsuzaki Y, Ohno K, Saya H (2009) Reversible whole-organism cell cycle arrest in a living vertebrate. Cell Cycle 8: 620–627.

Sargent R (2009) Gigapixel Panoramas, Gigapan overview, Global Connection Project. Available at http://www.cs.cmu.edu/~globalconn/gigapan.html

Schnabel R, Hutter H, Moerman D, Schnabel H (1997) Assessing normal embryogenesis in *Caenorhabditis elegans* using a 4D microscope: Variability of development and regional specification. Developmental Biology 184: 234–265.

Schott R (2009) GigaPanner: Exploring the Creation and Uses of GigaPixel Images with a Focus on the GigaPan Project. Available at http://www.gigapanner.com

Schreckenberg GM, Jacobson AG (1975) Normal stages of development of the axolotl *Ambystoma mexicanum*. Developmental Biology 42: 391–400.

Sims MH, Dodson KE (2008) Gigapan as a tool for scientific collaborations. Abstract #IN41B-1148. In: American Geophysical Union, Fall Meeting 2008. Available at http://adsabs.harvard.edu/abs/2008AGUFMIN41B1148S

Smith JJ, Putta S, Walker JA, Kump DK, Samuels AK, Monaghan JR, Weisrock DW, Staben C, Voss SR (2005) Sal-Site: Integrating new and existing ambystomatid salamander research resources. BMC Genomics 6: 181.

Tsang CKG, Kler (2002) 3D Imaging of Spherical Objects. Undergraduate Thesis. Winnipeg: Department of Electrical and Computer Engineering, University of Manitoba.

Twitty VC (1928) Experimental studies on the ciliary action of amphibian embryos. Journal of Experimental Zoology 50: 319–344.

Ubbels GA, Hara K, Koster CH, Kirschner MW (1983) Evidence for a functional role of the cytoskeleton in determination of the dorsoventral axis in *Xenopus laevis* eggs. Journal of Embryology and Experimental Morphology 77: 15–37.

Uretz RB, Bloom W, Zirkle RE (1954) Irradiation of parts of individual cells II. Effects of an ultraviolet microbeam focused on parts of chromosomes. Science 120: 197–199.

Wang P, Hayden S, Masui Y (2000) Transition of the blastomere cell cycle from cell size-independent to size-dependent control at the midblastula stage in *Xenopus laevis*. Journal of Experimental Zoology 287: 128–144.

Webb SE, Miller AL (2003) Imaging intercellular calcium waves during late epiboly in intact zebrafish embryos. Zygote 11: 175–182.

Wilson PA, Keller RE (1991) Cell rearrangement during gastrulation of *Xenopus*: Direct observation of cultured explants. Development 112: 289–300.

Wolfe MF, Goldberg R (2000) Rube Goldberg: Inventions. New York: Simon and Schuster.

Yoneda M, Kobayakawa Y, Kubota HY, Sakai M (1982) Surface contraction waves in amphibian eggs. Journal of Cell Science 54: 35–46.

Zimmermann T, Siegert F (1998) 4D confocal microscopy of *Dictyostelium discoideum* morphogenesis and its presentation on the Internet. Development Genes and Evolution 208: 411–420.